DOI: 10.1002/ejic.200500706

The Synthesis and Characterisation of Bis(phosphane)-Linked (η^6-*p*-Cymene)-ruthenium(II)–Borane Compounds

Adrian B. Chaplin,[a] Rosario Scopelliti,[a] and Paul J. Dyson*[a]

Keywords: Ruthenium / P ligands / Bridging ligands / Coordination modes / Boranes

The reaction of $[(\eta^6\text{-}p\text{-cymene})RuCl_2]_2$ with some bis(phosphane) ligands (dppm, dppe, dppv, dppa, dpp14b, dppf) has been investigated. In general mixtures of products were obtained, although the pendant phosphane complexes $[(\eta^6\text{-}p\text{-cymene})RuCl_2(\eta^1\text{-dppv})]$ and $[(\eta^6\text{-}p\text{-cymene})RuCl_2(\eta^1\text{-dppa})]$ were isolated and characterized in the solid state by X-ray diffraction. The later complex was obtained in lower yield and undergoes an equilibration reaction resulting in the formation of a dimeric species, where the dppa bridges two ruthenium centres, and uncoordinated phosphane; the bridging species was also structurally characterised in the solid state. In contrast, the reaction of $[(\eta^6\text{-}p\text{-cymene})RuCl_2(PPh_3)]$ with dppa in the presence of $[NH_4]PF_6$ results in the formation of $[(\eta^6\text{-}p\text{-cymene})RuCl(PPh_3)(\eta^1\text{-dppa})]PF_6$, which is stable in solution. A series of linked ruthenium–borane complexes, viz. $[(\eta^6\text{-}p\text{-cymene})RuCl_2(\eta^1\text{-phosphane-}BH_3)]$ (phosphane = dppm, dppe, dppv, dppa, dpp14b, dppf) and $[(\eta^6\text{-}p\text{-cymene})RuCl(PPh_3)(\eta^1\text{-dppa-}BH_3)]PF_6$ have been prepared from isolated pendant phosphane complexes, those generated in situ, or from a preformed phosphane–borane adduct. The solid-state structures of $[(\eta^6\text{-}p\text{-cymene})RuCl_2(\eta^1\text{-dppm-}BH_3)]$, $[(\eta^6\text{-}p\text{-cymene})RuCl_2(\eta^1\text{-dppe-}BH_3)]$ and $[(\eta^6\text{-}p\text{-cymene})RuCl_2(\eta^1\text{-dppv-}BH_3)]$ have been determined by X-ray diffraction analysis.

Introduction

The use of chelating phosphane ligands is prevalent in the coordination chemistry of the transition metals,[1] with complexes incorporating chelating phosphane ligands finding many applications in catalysis, where the versatility of this ligand class has allowed the rational design of highly active and selective compounds.[2] Bis(phosphane) ligands can also be found to bridge metal centers and coordinate selectively through one phosphorus centre, leading the other end free.[3–5] Such pendant coordination provides a way to link a variety of fragments, including simple metal complexes, metal cluster compounds, and main group fragments.[3c–g,4,6]

Ruthenium(II) complexes have well documented catalytic utility in organic chemistry,[2d] among which half sandwich (η^6-arene)ruthenium(II) complexes constitute an important class. As part of our continuing investigation of these complexes for catalytic hydrogenation reactions,[7] we have embarked on developing methodologies for the preparation of compounds in which the catalytically active ruthenium fragment is linked to other metal and non-metal moieties. These include functionalisation of the coordinated arene with imidazolium groups or crown ether moieties,[8] and formation of a heterometallic carbene complex.[9] In this paper we describe the preparation of model-linked (η^6-*p*-cymene)-ruthenium(II) systems using bis(phosphane) ligands.

For these linked systems the borane moiety, BH_3, was selected as a model-linked species as phosphane–borane adducts are formed rapidly and tend to be thermally stable.[10] Furthermore, coordination of a phosphane to BH_3 is a common method for protecting valuable (usually chiral) phosphanes from oxidation, either during storage or during synthetic transformations.[10] Phosphane–borane adducts have also been used as bidentate ligands, coordinating through a P centre and agostic B–H interactions (**a**,[11] **b**,[12] **c**–**e**[13] in Figure 1). In addition, as models for metalloborane ruthenium clusters, Barton and co-workers have previously prepared $[(\eta^6\text{-}p\text{-cymene})RuCl_2PPh_2CH_2C_6H_4\text{-}CH_2PPh_2BH_3]$ (**f**) and $[(\eta^6\text{-}p\text{-cymene})RuCl_2PPh_2(CH_2)_6\text{-}PPh_2BH_3]$ (**g**) from the reaction of either isolated or in-situ generated (η^6-*p*-cymene)ruthenium pendant phosphane complexes with BH_3·THF.[4]

Results and Discussion

The direct reaction between $[(\eta^6\text{-}p\text{-cymene})RuCl_2]_2$ and bis(phosphane) ligands in a 1:2 ratio generally results in the formation of the desired pendant phosphane complexes, viz. $[(\eta^6\text{-}p\text{-cymene})RuCl_2(\eta^1\text{-phosphane})]$, together with other ruthenium-containing species. In the case of potentially chelating phosphane ligands, formation of the η^2-coordinated complex, presumably following initial η^1-coordination followed by intramolecular chloride substitution,

[a] Institut des Sciences et Ingénierie Chimiques, Ecole Polytechnique Fédérale de Lausanne (EPFL),
1015 Lausanne, Switzerland
E-mail: paul.dyson@epfl.ch

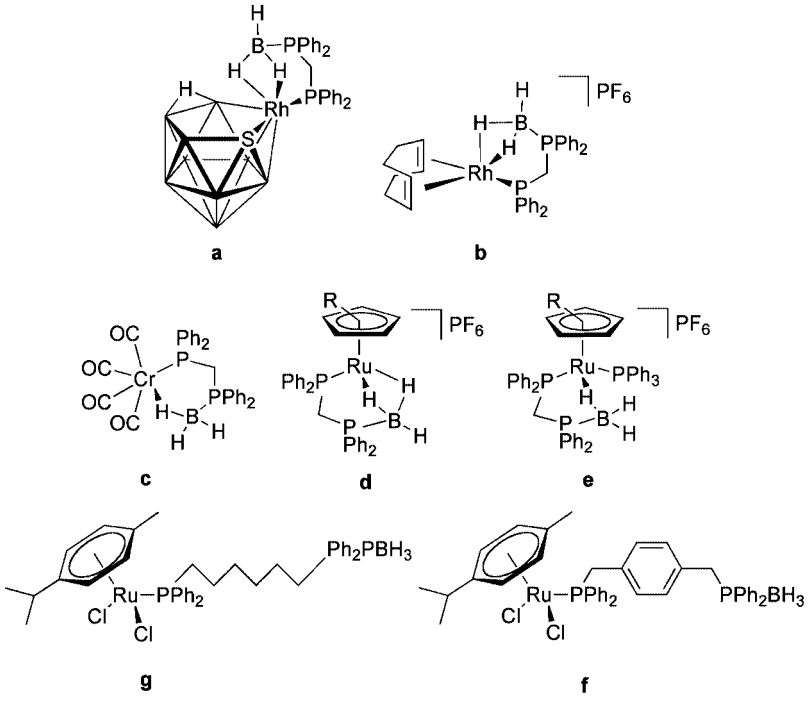

Figure 1. Examples of metal-containing phosphane–borane adducts.

can be suppressed by avoiding polar solvents, such as methanol and ethanol, which promote chloride loss. In such a way the previously reported complex [(η^6-*p*-cymene)-$RuCl_2$(η^1-dppm)] (**1**) has been prepared in high yield (76%) [7a] using benzene as a solvent.[5,7a] However, reaction of the phosphane ligands investigated in this report, see Figure 2, even in large excess, with [(η^6-*p*-cymene)$RuCl_2$]$_2$ in dichloromethane generally resulted in the formation of mixtures composed of the η^1-coordinated phosphane complex and a linked ruthenium–ruthenium complex where the phosphane ligand bridges the two metal centres. The *cis*-bis(1,2-diphenylphosphanyl)ethylene (dppv) ligand was, however, a notable exception to this generalisation, forming only the desired pendant phosphane complex [(η^6-*p*-cymene)-$RuCl_2$(η^1-dppv)] (**2**) in 89% yield using a stoichiometric phosphane to ruthenium ratio. The η^1-coordination mode is clearly evidenced by the presence of two doublets at δ = 15.1 and –30.6 ppm ($^3J_{PP}$ = 9.1 Hz) in the ^{31}P NMR spectrum, with the high-frequency resonance corresponding to the coordinated P centre. Selected NMR spectroscopic data for **2** and the other compounds described herein are listed in Table 1.

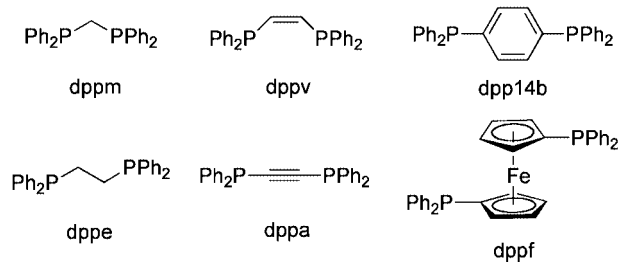

Figure 2. Bis(phosphane)s used in this study with their abbreviations.

To provide a possible explanation for the selective formation of these pendant phosphane complexes the solid-state structures of **2** and the oxide derivative of **1**, [(η^6-*p*-cymene)-$RuCl_2$(η^1-dppmO)] (**3**), obtained by slow oxidation of **1** in solution over a period of months,[16] were determined by X-

Table 1. Selected ^{31}P and ^{11}B NMR spectroscopic data.[a]

	Noncoordinated	Pendant phosphane complex			Bridged	Phosphane–borane complex			
		Ru–*P*	pend-*P*	J_{PP}	Ru–*P*	Ru–*P*	*P*BH_3	J_{PP}	P*B*H_3
dppm	–22.4	26.1[5c]	–27.6[5c]	31.8	21.1[14]	22.7	11.9	33.5	–38.4
dppe	–12.5	25.5	–12.6	34.8	22.5[7a]	23.6	18.2	42.8	–40.6
dppv	–23.1	15.1	–30.6	9.1	12.0	18.4[b]	9.2[b]	12.9[b]	–37.3[b]
dppa	–32.0	0.4[b]	–34.2[b]	3.6[b]	10.1[15]	3.2[b]	5.8[b]		–37.3[b]
PPh_3*dppa*	–32.0	1.0	–31.7	4.0	29.7,–2.8[c]	5.7	7.8		–37.7
dppf	–17.2	19.0	–17.6		18.3[14]	18.5	15.8		–38.5
dpp14b	–5.6	24.2	–5.2		24.6	24.9	20.5		–38.1

[a] $CDCl_3$, 298 K. Chemical shifts in ppm and coupling constants, *J*, in Hz. [b] 248 K. [c] $^2J_{PP}$ = 56.9 Hz.

ray diffraction analysis (see Figure 3 and Figure 4). The solid-state structure of **3** is much the same as that of **1**,[5b,5c] and the related pendant oxide complex [(η^6-*p*-cymene)-$RuCl_2\{\eta^1$-$PPh_2PCH(CH_3)P(O)Ph_2\}$] (**4**).[17] Each adopt the expected "piano-stool" geometries, with the phosphane chelate angle directed away from the chloride ligands. The Ru–P bond length in **3** is similar to that in **1** [2.355(7) vs. 2.368(7)[5b] Å], and the P–O bond in **3** is comparable with that in **4** [1.49(1) vs. 1.484(3) Å]. The structure of **2** bears close resemblance to **1** and **3** in many respects including the conformation of phosphane with respect to the ruthenium arene moiety and the Ru–P bond length [2.362(2) Å]. Of particular relevance to the reactivity of the pendant phosphane is the close proximity of the P centres in both **2** and **3** (and **1**). In the case of **2**, with a P···P distance of 3.481(3) Å, the close approach originates from the *cis* conformation of the alkene backbone, whereas in **3** the close approach [3.173(6) Å – averaged over the asymmetric cell, cf. **1**, 3.138(2) Å][5b] is a consequence of the small chelate angle [120.6(7)°]. These constraints provide a satisfactory explanation for the selective formation of the pendant phosphane complexes for dppm and dppv, as the steric bulk from the coordinated phosphane moieties, notably from the phenyl groups, can act to hinder further coordination.

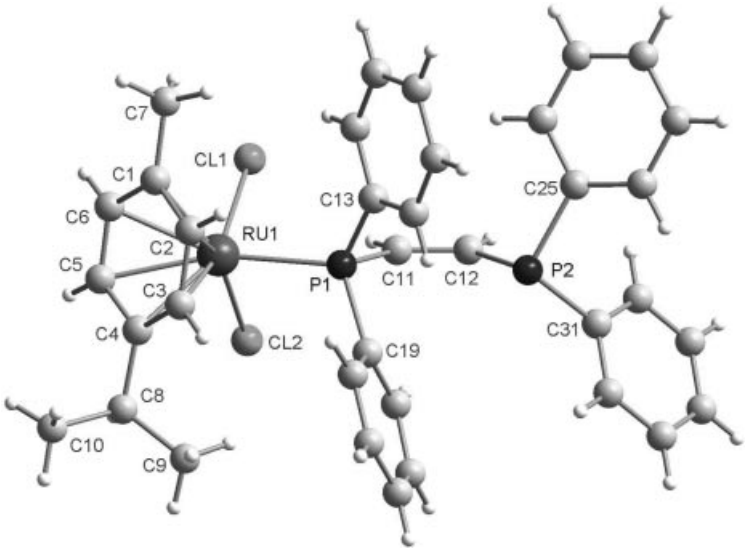

Figure 3. Ball-and-stick depiction of **2** in the solid state. Key bond lengths [Å] and angles [°]: Ru1–Cl1, 2.438(2); Ru1–Cl2, 2.418(1); Ru1–P1, 2.362(2): Cl1–Ru1–Cl2, 89.26(5); Cl1–Ru1–P1, 86.82(6); Cl2–Ru1–P1, 82.58(5); Ru1–C_{avg}, 2.21(3); Ru1–centroid, 1.7002(4); P1–C11, 1.833(5); P2–C12, 1.845(5); C11–C12, 1.336(7); P1–C11–C12, 126.9(4); P2–C12–C11, 124.4(4).

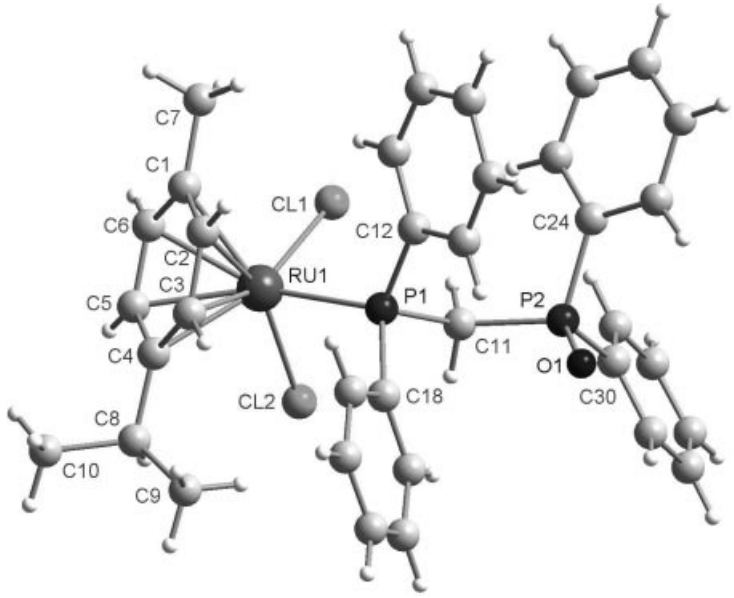

Figure 4. Ball-and-stick depiction of **3** in the solid state [selected molecule from the asymmetric cell]. Key bond lengths [Å] and angles [°] [averaged over asymmetric cell]: Ru–Cl, 2.432(7); Ru–Cl′, 2.420(3); Ru–P, 2.355(7): Cl–Ru–Cl′, 88.7(9); Cl–Ru–P, 87.2(9); Cl′–Ru–P, 83.4(8); Ru–C_{avg}, 2.21(2); Ru–centroid, 1.700(5); P–C, 1.84(2); P′–C, 1.82(1); P–C–P′, 120.6(7); P′–O, 1.49(1).

The competing formation of the bridged diruthenium species, by coordination of the pendant P centre to another ruthenium unit, encumbers the isolation of the desired pendant phosphane complexes. For example, the pendant phosphane complex, [(η^6-*p*-cymene)$RuCl_2$(η^1-dppa)] (**5**) was separated from the corresponding bridged species [(η^6-*p*-cymene)$RuCl_2$(μ-dppa)$RuCl_2$(η^6-*p*-cymene)] (**6**), in ca. 17% yield, following successive recystallisations from dichloromethane/pentane at –20 °C. Compound **5** is, however, unstable at room temperature and undergoes an equilibration reaction, liberating free phosphane and generating the bridged species **6**, as depicted in Scheme 1. After ca. 1 day in $CDCl_3$ an equilibrium composition is reached, corresponding to an equilibrium constant of $K = 0.42$ (Figure 5). Likewise, this equilibration can also be effected starting from **6** and dppa (≈ 1:1) on a similar timescale (ca. 1 day at room temperature in $CDCl_3$). Both these reactions follow first-order reaction kinetics, consistent with a mechanism involving dissociation of dppa and formation of the coordinately unsaturated arene ruthenium species "[(η^6-*p*-cymene)-$RuCl_2$]", as depicted in Scheme 1. An alternative proposal in which chloride dissociation leads to the intermediate species [(η^6-*p*-cymene)$RuCl_2$(η^1-dppa){(μ-dppa)$RuCl_2$(η^6-*p*-cymene)}]$^+$, moderately stable in solution,[18] can be dismissed because it was not detected by NMR spectroscopy during the equilibration process.

Using toluene as the solvent instead of dichloromethane for the reaction between [(η^6-*p*-cymene)$RuCl_2$]$_2$ and dppa (1.1 equiv. per Ru, room temperature), **6** selectively precipitates on formation, driving the equilibrium to the right hand side, resulting in a **5**/**6** product distribution of ca. 2 compared to the equilibrium ratio of 0.63.[19] The reaction was also carried out in dichloromethane at –78 °C with an excess of phosphane (2.3 equiv. per Ru). The resultant ratio of **5**/**6** was ca. 0.2, as determined by ^{31}P NMR spectroscopy, much lower than that of the equilibrium composition. Below –50 °C the rate of formation of **6** is slow enough to allow NMR characterisation of **5**. The ^{31}P NMR spectrum (as for complex **2**) displays the characteristic pair of doublets, with the coordinated phosphane resonance at $\delta = 0.4$ and the pendant P centre at $\delta = -34.2$, although the coupling constant, $^3J_{PP}$, is reduced in comparison to **2** [9.1 vs. 3.6 Hz]. The solid-state structures of **5** and **6** have been determined by X-ray diffraction analysis, and are depicted in Figure 6 and Figure 7, respectively. Each have "pianostool" geometries about the Ru centres, although as sug-

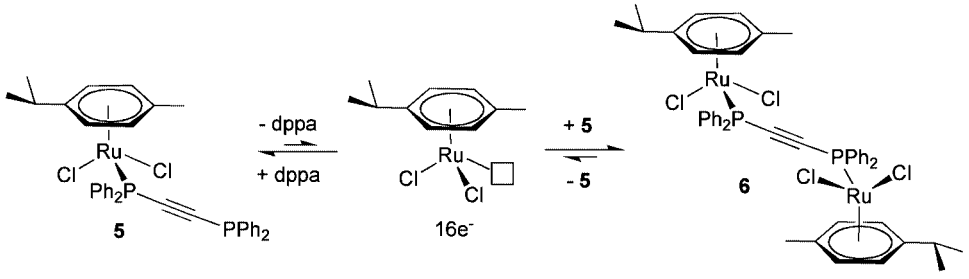

Scheme 1. Proposed mechanism for the equilibration of [(η^6-*p*-cymene)$RuCl_2$(η^1-dppa)] (**5**) with [(η^6-*p*-cymene)$RuCl_2$(μ-dppa)$RuCl_2$(η^6-*p*-cymene)] (**6**).

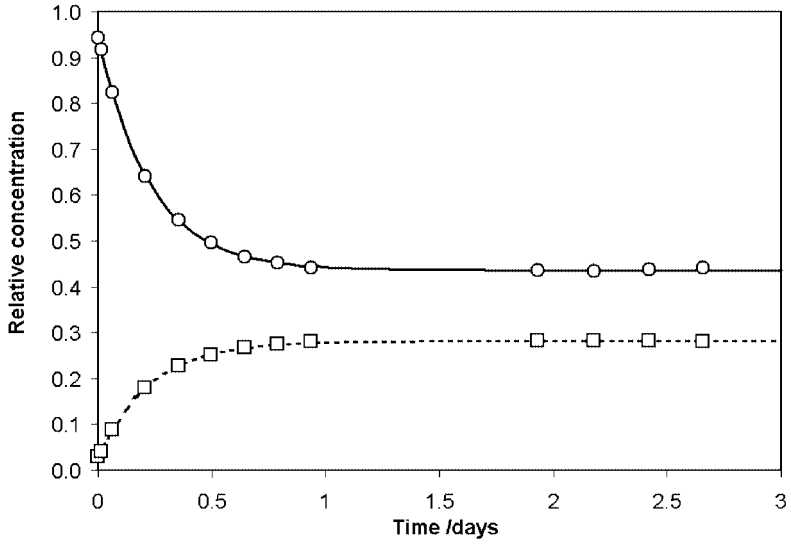

Figure 5. Equilibrium between complexes **5** and **6** at room temperature in $CDCl_3$. Relative concentrations of **5** (circles) and **6** (squares) were determined by integration of ^{1}H NMR spectroscopic data. Note, the concentration of dppa is not shown as it is identical to that of **6**.

gested by the difference in the coordinated phosphane resonances [**5**, δ = 0.4; **6**,[15] δ = 10.1] there are slight differences in the coordination sphere geometries. In particular the Ru–P bond in **5**, is elongated in comparison to **6** [2.336(1) vs. 2.319(1) Å] together with increased Cl–Ru–P angles [87.18(8) vs. 85.1(7)°] and a reduced Cl–Ru–Cl angle [86.08(4) vs. 88.10(4)°]. These differences are likely to originate from the steric constraints present in **6** owing to the rigid backbone of the dppa ligand, which deviates from linearity slightly more in **6**.

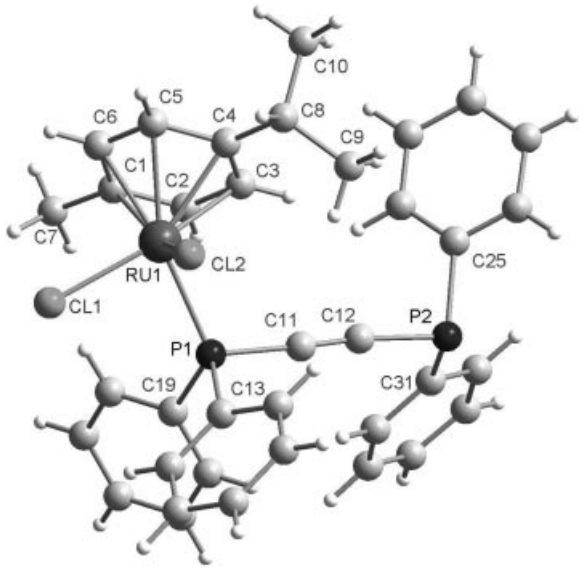

Figure 6. Ball-and-stick depiction of **5** in the solid state. Key bond lengths [Å] and angles [°]: Ru1–Cl1, 2.418(1); Ru1–Cl2, 2.402(1); Ru1–P1, 2.336(1): Cl1–Ru1–Cl2, 86.08(4); Cl1–Ru1–P1, 87.12(5); Cl2–Ru1–P1, 87.24(5); Ru1–C_{avg}, 2.21(2); Ru1–centroid, 1.7006(5); P1–C11, 1.782(5); P2–C12, 1.765(6); C11–C12, 1.202(7); P1–C11–C12, 175.1(5); P2–C12–C11, 174.0(5).

To further investigate the coordination chemistry of dppa it was reacted with the monosubstituted triphenylphosphane derivative [(η^6-*p*-cymene)$RuCl_2(PPh_3)$] together with one equivalent of $[NH_4]PF_6$ in methanol, resulting in the selective formation of the cationic pendant phosphane complex [(η^6-*p*-cymene)$RuCl(PPh_3)$(η^1-dppa)]PF_6 (**7**). The proposed structure was unambiguously identified by NMR spectroscopy, ES-MS and elemental analysis. The ^{31}P NMR spectrum shows three distinct phosphane resonances; a high-frequency doublet at δ = 24.2 ppm (Ru–*P*Ph_3, $^2J_{PP}$ = 55.1 Hz), a doublet of doublets at δ = 1.0 (Ru–*P*Ph_2CCPPh_2, $^2J_{PP}$ = 55.1, $^3J_{PP}$ = 3.2 Hz), and low frequency doublet at δ = –31.7 ppm corresponding to the pendant P centre ($^3J_{PP}$ = 4.9 Hz), in accordance with the proposed structure. In contrast to **5**, the cationic complex **7** is stable in solution over long periods of time, as evidenced by no discernible changes in its ^{31}P NMR spectrum after ca. 3.5 days in $CDCl_3$ solution. In **7** the signal of the quaternary carbon of the isopropyl group at the *p*-cymene ring (C^4 in Figure 8) is located at δ = 129.7 ppm by ^{1}H,^{13}C long-range correlation NMR spectroscopy, ca. 20 ppm to higher frequency than in **5** and **6** (and also to the other ruthenium complexes). This is indicative of weaker coordination to the metal centre, presumably from the increased steric bulk in the ruthenium coordination sphere. The ES-MS spectrum recorded in MeOH exhibits a strong molecular ion peak at *m*/*z* +927 with the expected isotope pattern. Structural information was obtained by selective fragmentation[20] of the parent peak resulting primary in loss of the PPh_3 ligand.

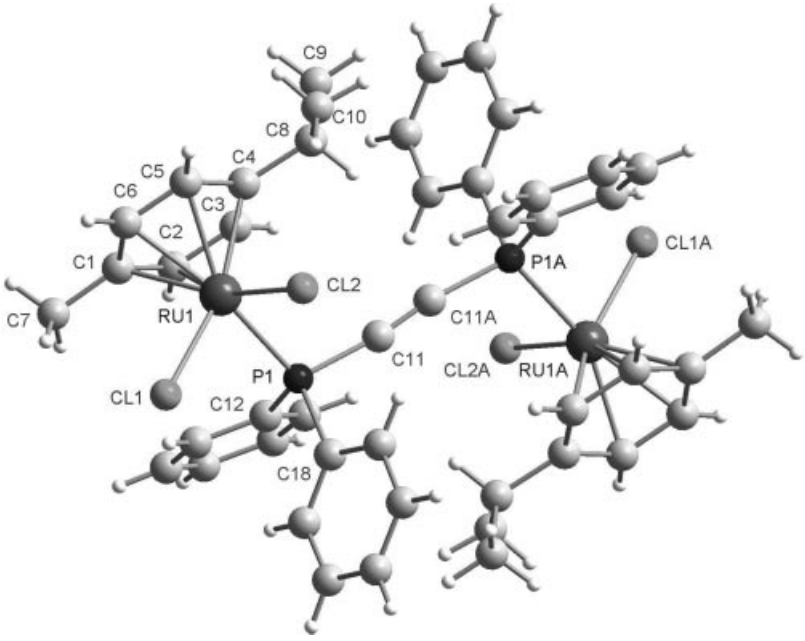

Figure 7. Ball-and-stick depiction of **6** in the solid state. Symmetry equivalent atoms, labeled with an A, are obtained by the symmetry operation –*x*, –*y*, 2 – *z*. Key bond lengths [Å] and angles [°]: Ru1–Cl1, 2.403(1); Ru1–Cl2, 2.204(1); Ru1–P1, 2.319(1): Cl1–Ru1–Cl2, 88.10(4); Cl1–Ru1–P1, 84.56(4); Cl2–Ru1–P1, 85.56(4); Ru1–C_{avg}, 2.22(3); Ru1–centroid, 1.7045(3); P1–C11, 1.762(4); C11–C11#, 1.207(8); P1–C11–C11#, 172.4(5).

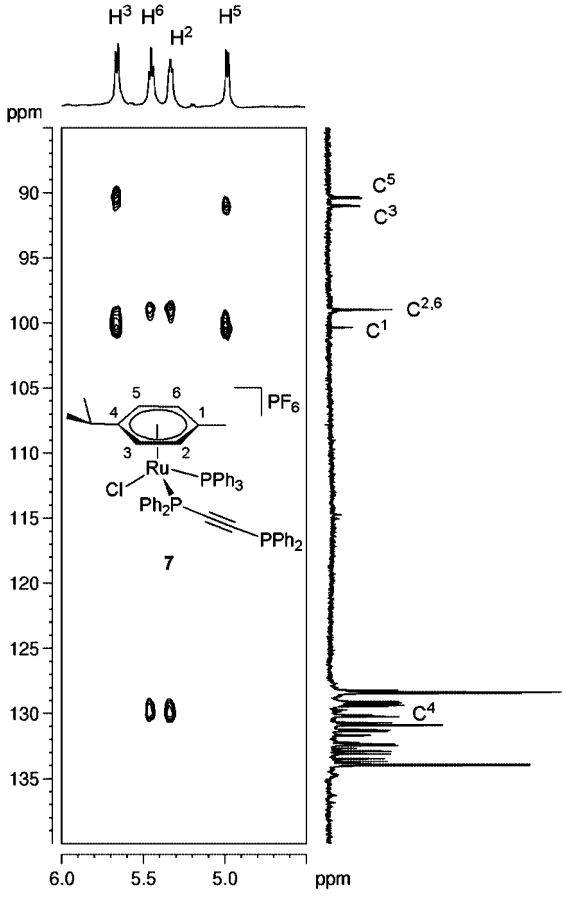

Figure 8. Section of the $^1H,^{13}C$ long-range correlation NMR spectrum of **7**. Cross peaks originate from $^3J_{CH}$ couplings ($CDCl_3$, room temperature).

Synthesis and Characterisation of Ruthenium–Borane Adducts

The isolated pendant phosphane complexes, **1**, **2**, **5** and **7**, react readily with BH_3·THF to give the corresponding ruthenium–borane adducts, **1B**, **2B**, **5B** and **7B**, in good yield as depicted in Scheme 2. For complexes **5** and **7**, it was necessary to carry out the reaction at –78 °C to prevent hydroboration of the alkyne moiety. Similarly, complexes **8B** (dppe) and **9B** (dppf) can be prepared by reaction of BH_3·THF with the corresponding pendant phosphane complexes formed, instead, in situ (Scheme 3). Partial separation from the corresponding bridging species, formed in parallel to the pendant phosphane complexes, can be achieved by extraction of the solid residue with toluene and recyrstallisation from dichloromethane/pentane, although chromatography is necessary for complete separation.

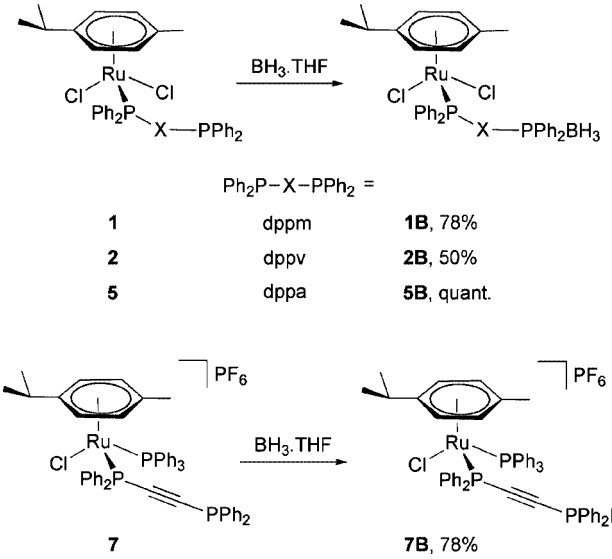

Scheme 2. Preparation of **1B**, **2B**, **5B** and **7B**.

A high-yielding method for the preparation of the ruthenium–borane species linked with the 1,4-bis(diphenylphosphanyl)benzene ligand (dpp14b) has been devised. The route, depicted in Scheme 4, involves the reaction of a preformed phosphane–borane, prepared in good yield (61%, 2 steps) from 1,4-bromo(diphenylphosphane)benzene, directly with $[(\eta^6$-*p*-cymene)$RuCl_2]_2$ (82% yield).

Large shifts of ca. δ = 35 ppm (see Table 1) and characteristic line broadening of the pendant P-centre resonances are observed in the ^{31}P NMR spectra for the ruthenium–borane complexes, although the frequencies of the coordinated P-centre resonances remain similar. Distinctive resonances at ca. δ = –38 ppm in the ^{11}B NMR spectra (see Table 1) are in agreement with related, previously reported, phosphane–borane adducts.[4] ^1H and ^{13}C NMR spectroscopic data for complexes **1B**, **2B**, **5B**, and **7B** are comparable with those of the isolated pendant phosphane complexes. In particular, the signal of the isopropyl quaternary carbon of the *p*-cymene ring in **7B** is similarly located at high frequency (δ = 131 ppm) as observed for **7**. The ES-MS spectrum of **7B** in MeOH exhibits a peak at *m*/*z* +927 resulting from loss of BH_3. If dichloromethane is used instead, the molecular ion peak at *m*/*z* +941 is observed to-

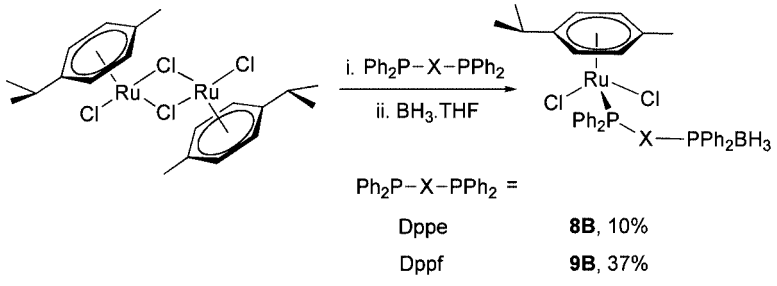

Scheme 3. Preparation of **8B** and **9B**.

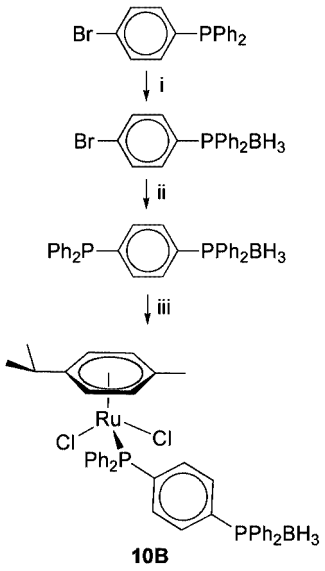

Scheme 4. Stepwise preparation of **10B**. Reagents and conditions: i. BH_3·THF, 0 °C; ii. BuLi, –78 °C, followed by $ClPPh_2$; iii. $[(\eta^6\text{-}p\text{-cymene})RuCl_2]_2$, room temp.; overall yield: 50%.

gether with a weaker peak at *m/z* +927. MS/MS of the parent peak correspondingly results in loss of BH_3, further selective fragmentation of this peak results resulting primary in loss of the PPh_3 ligand as for **7**.

Spectroscopic data for complexes **8B**, **9B** and **10B** corroborate the structure of the complexes well. Using NOESY it was possible to unambiguously determine the conformation of the dppf ligand in solution in **9B**, as depicted in Figure 9. In this conformation, the ferrocenyl rings adopt the expected antiperiplanar configuration, with both the borane moiety and ruthenium centre directed away from the ligand.

The solid-state structures of the complexes **1B**, **2B** and **8B** have been determined by X-ray diffraction analysis and are depicted in Figure 10, Figure 11 and Figure 12. Complexes **1B** and **2B** retain similar conformations as their parent pendant phosphane complexes **1**[5b] (also **3**, Figure 4) and **2** (Figure 3), although in both cases Ru–P bond lengths are slightly contracted in the borane adducts [2.351(2) vs. 2.368(7) Å for dppm; 2.3424(8) vs. 2.362(2) Å for dppv]. The structure of complex **8B** exhibits similar bonding parameters around the ruthenium centre to those observed in the related bridging species $[(\eta^6\text{-}p\text{-cymene})Ru(S_2C_2\{B_{10}H_{10}\})(\mu\text{-dppe})Ru(S_2C_2\{B_{10}H_{10}\})(\eta^6\text{-}p\text{-cymene})]$.[21] The P–B bond lengths range from 1.91–1.93 Å and are comparable to other phosphane–BH_3 adducts.[4,12,13]

In conclusion, a series of neutral bis(phosphane)-linked ruthenium–borane complexes have been prepared using a variety of phosphane ligands. While the use of isolated pendant phosphane complexes is more desirable and higher yielding, the formation of these complexes is usually accompanied by the formation of dimeric ruthenium–ruthenium species. In the case of the reaction between bis(diphenylphosphanyl)acetylene (dppa) and $[(\eta^6\text{-}p\text{-cymene})RuCl_2]_2$, equilibration between these two species occurs in

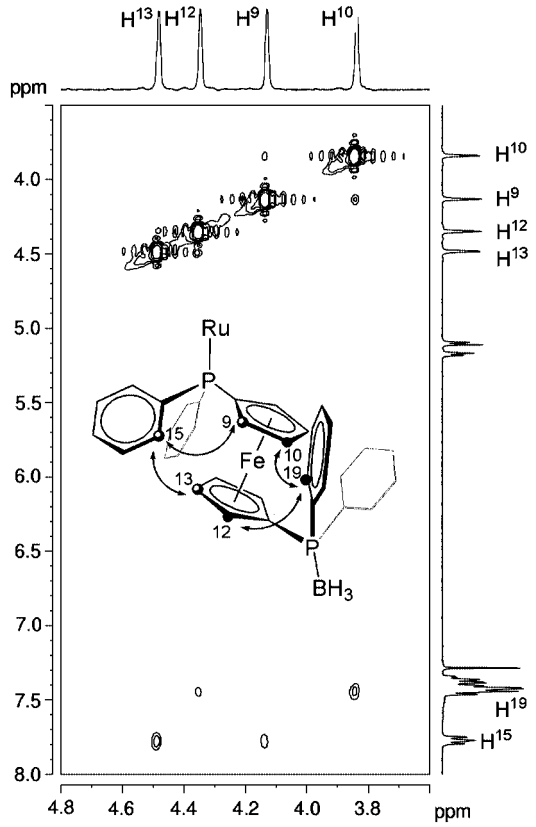

Figure 9. Section of the NOESY spectrum of **9B** ($CDCl_3$, room temperature).

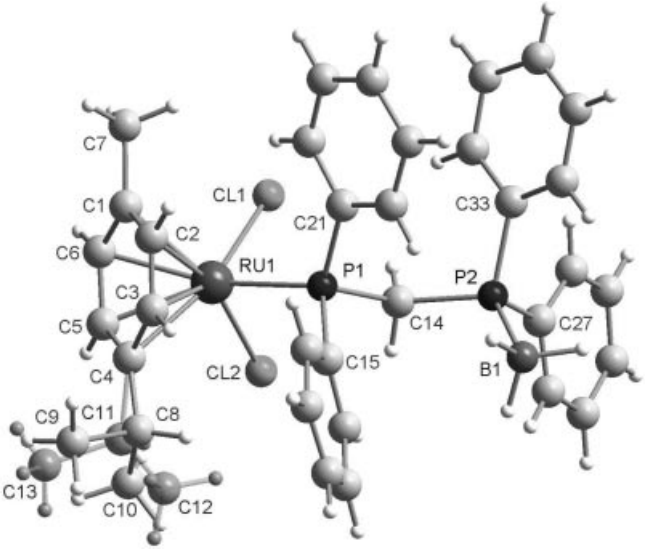

Figure 10. Ball-and-stick depiction of **1B** in the solid state. The minor disordered component of the *p*-cymene ring is composed of atoms C11–C13. Key bond lengths [Å] and angles [°]: Ru1–Cl1, 2.417(2); Ru1–Cl2, 2.393(2); Ru1–P1, 2.351(2): Cl1–Ru1–Cl2, 85.65(8); Cl1–Ru1–P1, 86.47(9); Cl2–Ru1–P1, 87.33(8); Ru1–C_{avg}, 2.19(3); Ru1–centroid, 1.7045(6); P1–C14, 1.831(8); P2–C14, 1.841(8); P1–C14–P2, 123.4(4); P2–B1, 1.91(1).

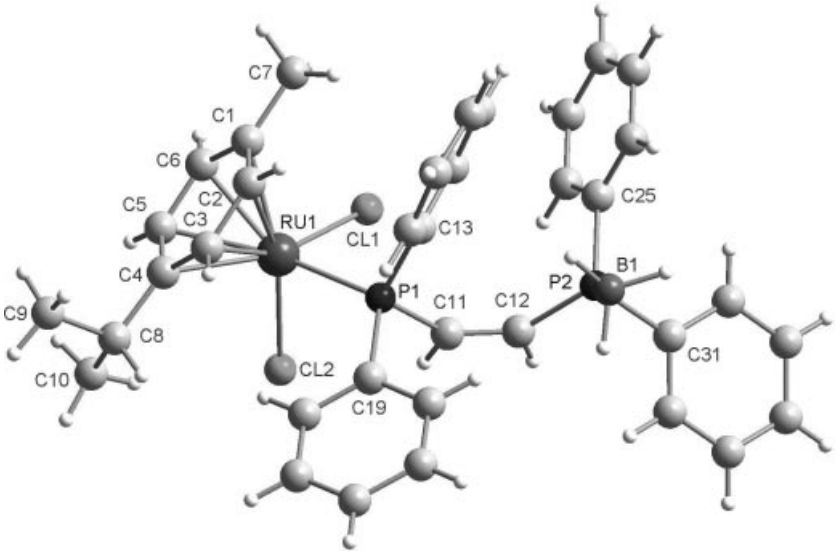

Figure 11. Ball-and-stick depiction of **2B** in the solid state. Key bond lengths [Å] and angles [°]: Ru1–Cl1, 2.4107(8); Ru1–Cl2, 2.4307(8); Ru1–P1, 2.3424(8): Cl1–Ru1–Cl2, 88.11(3); Cl1–Ru1–P1, 83.32(3); Cl2–Ru1–P1, 86.28(3); Ru1–C_{avg}, 2.22(4); Ru1–centroid, 1.7116(3); P1–C11, 1.823(3); P2–C12, 1.813(3); C11–C12, 1.327(4); P1–C11–C12, 139.3(3); P2–C12–C11, 135.3(3); P2–B1, 1.932(4).

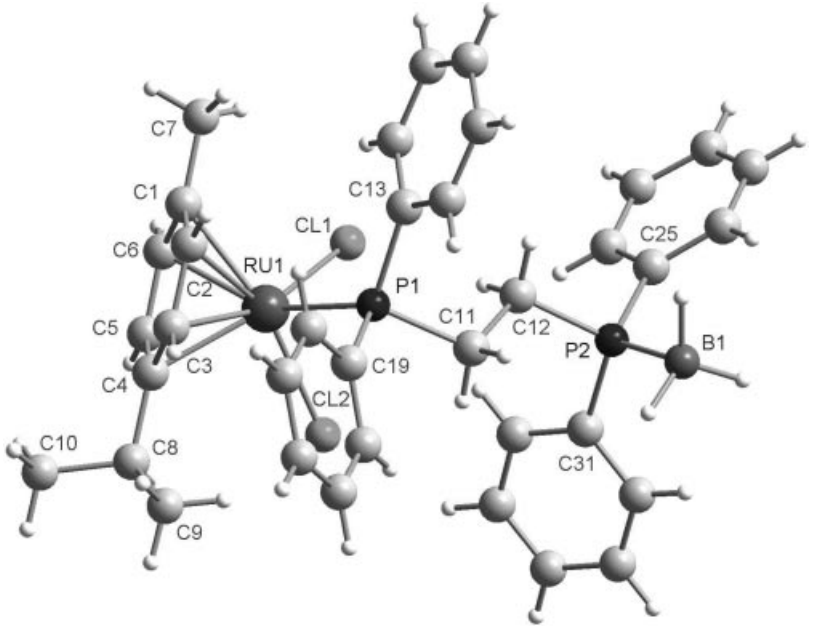

Figure 12. Ball-and-stick Depiction of **8B** in the solid state. Key bond lengths [Å] and angles [°]: Ru1–Cl1, 2.436(2); Ru1–Cl2, 2.413(2); Ru1–P1, 2.356(2): Cl1–Ru1–Cl2, 88.86(5); Cl1–Ru1–P1, 90.42(6); Cl2–Ru1–P1, 84.49(6); Ru–C_{avg}, 2.21(2); Ru1–centroid, 1.7005(5); P1–C11, 1.858(5); P2–C12, 1.817(6); C11–C12, 1.538(8); P1–C11–C12, 113.0(4); P2–C12–C11, 112.8(4); P2–B1, 1.933(8).

solution. In contrast, the reaction between *cis*-bis(1,2-diphenylphosphanyl)ethylene (dppv) and $[(\eta^6\text{-}p\text{-cymene})\text{-}RuCl_2]_2$ results in the selective formation of the pendant phosphane complex akin to dppm. These observations were rationalised by inspection of their solid-state structures (and related oxide and borane adducts), which show a close proximity between the P centres. In contrast for dppe and dppf the solid-state structure and solution conformation determined by NOESY, respectively, of the linked ruthenium–borane complexes are suggestive (vide infra) of little steric hindrance to further coordination. Correspondingly, the linked ruthenium–borane systems using these ligands are prepared in lower yield and require chromatographic purification. As an alternative methodology, a preformed phosphane–borane ligand was prepared preventing contamination from the corresponding bridging species.

Experimental Section

All organometallic manipulations were carried out under nitrogen using standard Schlenk techniques. CH_2Cl_2, diethyl ether, hexane, THF and toluene were dried using a solvent purification system,

manufactured by innovative technology inc., in which nitrogen-saturated solvents are passed through a series of alumina columns or, for the hydrocarbons, through one column of alumina then another containing a copper catalyst under a positive pressure of nitrogen. All other solvents were p. a. quality and saturated with nitrogen prior to use. Chromatographic separations were carried out in air using 1.0×20×20 mm silica gel 60 F_{254} plates (Merck). [(η^6-*p*-cymene)$RuCl_2$]$_2$,[22] [(η^6-*p*-cymene)$_2Ru_2(\mu$-Cl)$_3$]PF_6,[23] [(η^6-*p*-cymene)-$RuCl_2(PPh_3)$],[23] [(η^6-*p*-cymene)$RuCl_2(\eta^1$-dppm)],[7a] dpp14b,[24] and 1,4-bromo(diphenylphosphane)benzene,[24] were prepared as described elsewhere. All other chemicals are commercial products and were used as received. Spectra were recorded with a Bruker Avance 400 spectrometer at room temperature, unless otherwise stated. Chemical shifts are given in ppm and coupling constants (*J*) in Hz. ES mass spectra were recorded with a Thermo Finnigan LCQ DECA XPPlus and microanalyses performed at the EPFL. Numerical analysis for the equilibration of **5** – (**6** + dppa) was carried out using Origin 7.5 (OriginLab).

Preparation of [(η^6-*p*-Cymene)$RuCl_2(\eta^1$-*cis*-$PPh_2CHCHPPh_2$)] (2): A solution of [(η^6-*p*-cymene)$RuCl_2$]$_2$ (0.160 g, 0.26 mmol) and dppv (0.207 g, 0.26 mmol) in CH_2Cl_2 (50 mL) was stirred at room temperature for 1 h. The product was obtained as an orange solid following concentration and precipitation with diethyl ether. Yield 0.32 g (89%). Crystals suitable for X-ray crystallography were obtained by recrystallisation from CH_2Cl_2/diethyl ether at 4 °C. ^{1}H NMR ($CDCl_3$): δ = 8.1–8.2 [m, 4 H, RuP(*o*-C_6H_5)$_2$ {^{31}P@δ = 15.1} δ = 8.15, d, $^3J_{HH}$ = 7.2], 7.54 (ddd, $^3J_{HH}$ = 13.5, $^2J_{PH}$ = 28.5, $^3J_{PH}$ = 31.0 Hz, 1 H, $RuPPh_2CHCH$), 7.38–7.44 [m, 2 H, RuP(*p*-C_6H_5)$_2$], 7.30–7.38 [m, 4 H, RuP(*m*-C_6H_5)$_2$], 7.18–7.24 [m, 2 H, pend-P(*p*-C_6H_5)$_2$], 7.12–7.18 [m, 4 H, pend-P(*m*-C_6H_5)$_2$], 7.06 (ddd, $^3J_{PH}$= 13.5, $^2J_{HH}$ = 4.0, $^3J_{PH}$ = 38.1 Hz, 1 H, $CHCHPPh_2$), 6.85–6.95 [m, 4 H, pend-P(*o*-C_6H_5)$_2$ {^{31}P@δ = –30.6} δ = 6.91 dd, $^4J_{HH}$ = 1.2, $^3J_{HH}$ = 8.2 Hz], 5.26 (d, $^3J_{HH}$ = 5.1, 2 H, *o*-$CH_3C_6H_4$), 5.15 (d, $^3J_{HH}$ = 6.0, 2 H, *m*-$CH_3C_6H_4$), 2.55 [sept, $^3J_{HH}$ = 6.9 Hz, 1 H, $CH(CH_3)_2$], 1.84 (s, 3 H, CH_3–C_6H_4), 0.85 [d, $^3J_{HH}$ = 6.9 Hz, 6 H, $CH(CH_3)_2$] ppm. ^{13}C{^{1}H} NMR ($CDCl_3$): δ = 145.2 (dd, $^1J_{PC}$ = 7.6, $^2J_{PC}$ = 17.4 Hz, $CHCHPPh_2$), 140.3 (dd, $^1J_{PC}$ = 21.5, $^2J_{PC}$ = 44.4 Hz, $RuPPh_2CHCH$), 137.6 [d, $^1J_{PC}$ = 10.6, pend-P(*i*-C_6H_5)$_2$], 134.2 [d, $^1J_{PC}$ = 45.6, RuP(*i*-C_6H_5)$_2$], 133.5 [dd, $^4J_{PC}$ = 4.5, $^2J_{PC}$ = 9.7, RuP(*o*-C_6H_5)$_2$], 132.5 [d, $^2J_{PC}$ = 18.4, pend-P(*o*-C_6H_5)$_2$], 130.4 [d, $^4J_{PC}$ = 2.4, RuP(*p*-C_6H_5)$_2$], 128.2–128.4 [obscured, pend-P(*p*-C_6H_5)$_2$], 128.3 [d, $^3J_{PC}$ = 10.9, P(*m*-C_6H_5)$_2$], 128.2 [d, $^3J_{PC}$ = 10.0, P(*m*-C_6H_5)$_2$], 108.6 [s, $CCH(CH_3)_2$], 93.7 (s, CH_3–*C*), 90.3 (d, $^2J_{PC}$ = 4.2, *o*-$CH_3C_6H_4$), 85.2 (d, $^2J_{PC}$ = 6.0, *m*-$CH_3C_6H_4$), 30.1 [s, $CH(CH_3)_2$], 21.4 [s, $CH(CH_3)_2$], 17.4 (s, CH_3–C_6H_4) ppm. ^{31}P{^{1}H} NMR ($CDCl_3$): δ = 15.1 (d, $^3J_{PP}$ = 9.1 Hz, 1 P, Ru–*P*), –30.6 (d, $^3J_{PP}$ = 9.1 Hz, 1 P, pend-*P*) ppm. $C_{36}H_{36}Cl_2P_2Ru$ (702.60): calcd. C 61.54, H 5.16; found C 60.98, H 5.25.

Preparation of [(η^6-*p*-Cymene)$RuCl_2(\eta^1$-*cis*-$PPh_2CHCHPPh_2BH_3$)] (2B): To a solution of **2** (0.100 g, 0.14 mmol) in CH_2Cl_2 (15 mL, 0 °C) a solution of BH_3·THF in THF (0.12 mL of ca. 1.2 M, 0.14 mmol) was added dropwise. The solution was then warmed to room temperature and stirred for 1 h. The solvent was then removed in vacuo, and the solid washed with diethyl ether (25 mL) and then recrystallised from CH_2Cl_2/pentane at –20 °C to give red crystals suitable for X-ray diffraction. Yield: 0.05 g (50%) ^{1}H NMR ($CDCl_3$, –50 °C): δ = 7.9–8.1 [m, 4 H, RuP(*o*-C_6H_5)$_2$ {^{31}P@δ = 18.4} δ = 7.97, d, $^3J_{HH}$ = 7.3], 7.69 (ddd, $^3J_{HH}$ = 16.2, J_{PH} = 21.2, J_{PH} = 39.7, 1 H, PPh_2CH), 7.2–7.5 [m, 16 H, P(*o*-C_6H_5)$_2BH_3$ and P(*m*,*p*-C_6H_5)$_2$], 6.86 (ddd, J_{PH} = 4.7, $^3J_{HH}$ = 16.2, J_{PH} = 36.9, 1 H, PPh_2CH), 5.17 (d, $^3J_{HH}$ = 5.8, 2 H, *m*-$CH_3C_6H_4$), 5.11 (d, $^3J_{HH}$ = 5.9, 2 H, *o*-$CH_3C_6H_4$), 2.62 [sept, $^3J_{HH}$ = 6.6, 1 H, $CH(CH_3)_2$], 1.75 (s, 3 H, CH_3–C_6H_4), 0.83 [d, $^3J_{HH}$ = 6.7, 6 H, $CH(CH_3)_2$], 0.1–0.7 [br., 3 H, BH_3; {^{11}B@δ = –37.3} δ = 0.42, d, $^2J_{PH}$ = 16.3]. ^{13}C{^{1}H} NMR ($CDCl_3$, –50 °C): δ = 145.6 (d, $^1J_{PC}$ = 39.0, PPh_2CH), 133.8 [d, $^2J_{PC}$ = 10.0, RuP(*o*-C_6H_5)$_2$], 133.3–133.9 (obscured, PPh_2CH), 132.1 [d, $^2J_{PC}$ = 9.5, P(*o*-C_6H_5)$_2BH_3$], 131.4 [br., RuP(*p*-C_6H_5)$_2$], 131.2 [br., P(*p*-C_6H_5)$_2BH_3$], 130.7 [d, $^1J_{PC}$ = 47.5, P(*i*-C_6H_5)$_2$], 130.4 [d, $^1J_{PC}$ = 60.3, P(*i*-C_6H_5)$_2$], 128.9 [d, $^3J_{PC}$ = 10.2, P(*m*-C_6H_5)$_2$], 128.5 [d, $^3J_{PC}$ = 10.6, P(*m*-C_6H_5)$_2$], 109.7 [d, $^2J_{PC}$ = 1.8, $CCH(CH_3)_2$], 94 (m, CH_3–*C*), 89.7 (d, $^2J_{PC}$ = 2.8, *o*-$CH_3C_6H_4$), 85.9 (d, $^2J_{PC}$ = 5.4 *m*-$CH_3C_6H_4$), 30.4 [s, $CH(CH_3)_2$], 21.4 [s, $CH(CH_3)_2$], 17.8 (s, CH_3–C_6H_4). ^{31}P{^{1}H} NMR ($CDCl_3$, –50 °C): δ = 18.4 (d, $^3J_{PP}$ = 12.9, 1 P, Ru–*P*), 9.3–10.1 (m, 1P, *P*–BH_3). ^{11}B{^{1}H} NMR ($CDCl_3$, –50 °C): δ = –37.3 (br). IR (nujol, cm^{-1}): $\tilde{\nu}_{v(BH)}$ = 2448 (br), 2380 (sh). $C_{36}H_{39}BCl_2P_2Ru{\cdot}CH_2Cl_2$ (801.37): calcd. C 55.46, H 5.16; found C 55.65, H 5.33.

Oxidation of [(η^6-*p*-Cymene)$RuCl_2(\eta^1$-$PPh_2CH_2PPh_2$)]: Orange crystals of [(η^6-*p*-cymene)$RuCl_2(\eta^1$-dppmO)] (**3**) suitable for X-ray diffraction were obtained by recrystallisation of a reaction mixture containing [(η^6-*p*-cymene)$RuCl_2(\eta^1$-dppm)] over several months from chloroform/pentane at 4 °C. Alternatively, [(η^6-*p*-cymene)-$RuCl_2(\eta^1$-dppm)] can be quantitatively converted to **2** by treatment with H_2O_2 in THF. ^{1}H and ^{31}P NMR spectroscopic data were in agreement with the literature data.[17]

Preparation of [(η^6-*p*-Cymene)$RuCl_2(\eta^1$-PPh_2CCPPh_2)] (5): To a vigorously stirred solution of dppa (0.17 g, 0.43 mmol) in CH_2Cl_2 (15 mL, –78 °C) a solution of [(η^6-*p*-cymene)$RuCl_2$]$_2$ (0.10 g, 0.16 mmol) in CH_2Cl_2 (15 mL) was added rapidly. Following an additional 5 min stirring, the solvent was removed in vacuo at room temperature. The resultant orange solid material was an ca. 0.4:1.0:0.7 mixture of **6**/**5**/dppa as determined by ^{31}P NMR spectroscopy. Successive recrystallisation from CH_2Cl_2/pentane at –20 °C gave orange crystals of **5** in ca. 0.04 g (17%) yield. Crystals of **6** suitable for X-ray analysis were obtained by slow diffusion of pentane into a CH_2Cl_2 solution of the reaction mixture at room temperature, whereas those of **5** were obtained after successive recrystallisation of the reaction mixture from CH_2Cl_2/pentane at –20 °C. ^{1}H NMR ($CDCl_3$, –50 °C): δ = 7.97 [dd, $^3J_{HH}$ = 7.2, $^3J_{PH}$ = 11.5, 4 H, RuP(*o*-C_6H_5)$_2$], 7.6–7.9 [m, 4 H, pend-P(*o*-C_6H_5)$_2$], 7.3–7.6 [m, 12 H, P(*m*,*p*-C_6H_5)$_2$], 5.31 (d, $^3J_{HH}$ = 5.9, 2 H, *m*-$CH_3C_6H_4$), 5.22 (d, $^3J_{HH}$ = 5.6, 2 H, *o*-$CH_3C_6H_4$), 2.80 [sept, $^3J_{HH}$ = 6.5, 1 H, $CH(CH_3)_2$], 1.85 (s, 3 H, CH_3–C_6H_4), 1.04 [d, $^3J_{HH}$ = 6.6, 6 H, $CH(CH_3)_2$]. ^{13}C{^{1}H} NMR ($CDCl_3$, –50 °C): δ = 133.7 [m, P(*i*-C_6H_5)$_2$], 133.0–133.5 [m, P(*o*-C_6H_5)$_2$], 131.0 [s, RuP(*p*-C_6H_5)$_2$], 130.2 [s, pend-P(*p*-C_6H_5)$_2$], 129.3 [d, $^3J_{PC}$ = 8.0, P(*m*-C_6H_5)$_2$], 128.4 [d, $^3J_{PC}$ = 10.9, P(*m*-C_6H_5)$_2$], 109.6 [s, $CCH(CH_3)_2$], 96.1 (s, CH_3–*C*), 89.9 (d, $^2J_{PC}$ = 3.5, *o*-$CH_3C_6H_4$), 87.3 (d, $^2J_{PC}$ = 5.2, *m*-$CH_3C_6H_4$), 30.5 [s, $CH(CH_3)_2$], 22.0 [s, $CH(CH_3)_2$], 17.9 (s, CH_3–C_6H_4), the signals of $RuPPh_2CCPPPh_2$ were not unambiguously located. ^{31}P{^{1}H} NMR ($CDCl_3$, –50 °C): δ = 0.4 (s, 1 P, Ru–*P*), –34.2 (d, $^3J_{PP}$ = 3.6, 1 P, pend-*P*). IR (nujol, cm^{-1}): $\tilde{\nu}_{v(CC)}$ = 2110 (w).

Preparation of [(η^6-*p*-Cymene)$RuCl_2(\eta^1$-$PPh_2CCPPh_2BH_3$)] (5B): To a solution of **5** (0.007 g, 0.01 mmol) in THF (2 mL, –78 °C) a solution of BH_3·THF in THF (0.01 mL of ca. 1.2 M, 0.012 mmol) was added dropwise. The solution was then stirred for 1 h, and the solvent was removed in vacuo as the solution warmed to room temperature. Yield: quantitative (by ^{1}H NMR). ^{1}H NMR ($CDCl_3$, –50 °C): δ = 7.8–7.95 [m, 8 H, {^{31}P@δ = 3.2} δ = 7.90, d, RuP(*o*-C_6H_5)$_2$, $^3J_{HH}$ = 7.2; {^{31}P@δ = 5.8} δ = 7.88, d, P(*o*-C_6H_5)$_2$-BH_3, $^3J_{HH}$ = 7.3], 7.3–7.65 [m, 12 H, P(*m*,*p*-C_6H_5)$_2$], 5.36 (d, $^3J_{HH}$ = 6.0, 2 H, *m*-$CH_3C_6H_4$), 5.28 (d, $^3J_{HH}$ = 5.7, 2 H, *o*-$CH_3C_6H_4$), 2.75 [sept, $^3J_{HH}$ = 6.7, 1 H, $CH(CH_3)_2$], 1.86 (s, 3 H, CH_3–C_6H_4), 1.02 [d, $^3J_{HH}$ = 6.8, 6 H, $CH(CH_3)_2$], 1.0–1.6 [br., 3 H, BH_3;

{^{11}B@δ = –37.3} δ = 1.30, d, $^2J_{PH}$ = 17.0]. ^{13}C{^{1}H} NMR ($CDCl_3$, –50 °C): δ = 133.3 [d, $^2J_{PC}$ = 10.6, RuP(*p*-C_6H_5)$_2$], 132.7 [s, P(*p*-C_6H_5)$_2$$BH_3$], 132.4 [d, $^2J_{PC}$ = 11.6, P(*p*-C_6H_5)$_2$$BH_3$], 131.4 [s, RuP(*p*-$C_6H_5$)$_2$], 130 [d, $^1J_{PC}$ ca. 60, P(*i*-C_6H_5)$_2$], 129.6 [d, $^3J_{PC}$ = 11.3, P(*m*-C_6H_5)$_2$$BH_3$], 128.7 [d, $^3J_{PC}$ = 11.0, RuP(*m*-C_6H_5)$_2$], 126.7 [d, $^1J_{PC}$ = 64.6, P(*i*-C_6H_5)$_2$], 110.4 [s, *C*CH(CH_3)$_2$], 104.5 [dd, $^1J_{PC}$ = 65.7, $^2J_{PC}$ = 7.5, PC*C*P], 99.2 (dd, $^1J_{PC}$ = 89.4, $^2J_{PC}$ < 2, P*C*CP), 96.9 (s, CH_3–*C*), 90.0 (d, $^2J_{PC}$ = 3.5, *o*-$CH_3C_6H_4$), 87.4 (d, $^2J_{PC}$ = 5.6, *m*-$CH_3C_6H_4$), 30.5 [s, *C*H(CH_3)$_2$], 21.9 [s, CH(*C*H_3)$_2$], 17.9 (s, *C*H_3–C_6H_4). ^{31}P{^{1}H} NMR ($CDCl_3$, –50 °C): δ = 5.8 (br., 1 P, *P*BH_3), 3.2 (s, 1 P, Ru*P*). ^{11}B{^{1}H} NMR ($CDCl_3$): δ = –37.3 (br).

Preparation of [(η^6-*p*-Cymene)RuCl(PPh_3)(η^1-PPh_2CCPPh_2)]PF_6 (7): A suspension of [(η^6-*p*-cymene)$RuCl_2$(PPh_3)] (0.70 g, 1.23 mmol), $[NH_4]PF_6$ (0.20 g, 1.23) and dppa (0.49 g, 1.23 mmol) in MeOH (150 mL) was heated at 35 °C for 3 h. The solvent was removed in vacuo, and the residue taken up in a minimal amount of CH_2Cl_2. A small amount of (unidentified) solid material was removed by the addition of hexane and filtration. Removal of the solvent gave an orange oil that solidified under high vacuum. Yield: 0.74 g (56%). ^{1}H NMR ($CDCl_3$): δ = 7.97 [dd, $^3J_{HH}$ = 7.2, $^3J_{PH}$ = 12.3, 2 H, RuP(*o*-C_6H_5)$_2$CCPPh_2], 7.60–7.75 [m, 4 H, pend-P(*o*-C_6H_5)$_2$ and pend-P(*o*-C_6H_5')$_2$], 7.30–7.60 (m, 20 H, P*Ph*), 7.10–7.25 [m, 7 H, RuP(*m*-C_6H_5)$_3$ and RuP(*p*-C_6H_5')$_2$], 6.92 [td, $^4J_{PH}$ = 2.9, $^3J_{HH}$ = 7.7, 2 H, RuP(*m*-C_6H_5')$_2$CCPPh_2], 5.66 (d, $^3J_{HH}$ = 6.2, 1 H, *m*-$CH_3C_6H_4$), 5.42–5.48 [m, 1 H, *o*-$CH_3C_6H_4'$ {^{31}P@δ = 1.0} δ = 5.45, d, $^3J_{HH}$ = 6.3], 5.30–5.35 [m, 1 H, *o*-$CH_3C_6H_4$ {^{31}P@δ = 24.1} δ = 5.33, d, $^3J_{HH}$ = 6.4], 4.99 (d, $^3J_{HH}$ = 6.1, 1 H, *m*-$CH_3C_6H_4'$), 2.79 [sept, $^3J_{HH}$ = 6.9, 1 H, C*H*(CH_3)$_2$], 1.28 (s, 3 H, C*H*$_3$–C_6H_4), 1.23 [d, $^3J_{HH}$ = 6.4, 3 H, CH(C*H*$_3$)$_2$], 1.21 [d, $^3J_{HH}$ = 6.4, 3 H, CH(C*H*$_3'$)$_2$]. ^{13}C{^{1}H} NMR ($CDCl_3$): δ = 134.0 [d, $^2J_{PC}$ = 9.6, RuP(*o*-C_6H_5)$_3$], 133.6 [d, $^2J_{PC}$ = 21.8, pend-P(*o*-C_6H_5)$_2$ or pend-P(*o*-$C_6'H_5$)$_2$], 133.0 [d, $^2J_{PC}$ = 21.0, pend-P(*o*-$C_6'H_5$)$_2$ or pend-P(*o*-C_6H_5)$_2$], 132.5 [d, $^1J_{PC}$ = 47.9, P(*i*-C_6H_5)$_2$], 132.4 [d, $^2J_{PC}$ = 9.9, RuP(*o*-$C_6'H_5$)$_2$], 131.7 [d, $^4J_{PC}$ = 2.3, P(*p*-C_6H_5)$_2$], 131.3 [d, $^2J_{PC}$ = 10.8, RuP(*o*-C_6H_5)$_2$], 130.9 [d, $^4J_{PC}$ = 2.3, P(*p*-C_6H_5)$_3$], 130.5 [d, $^1J_{PC}$ = 47.4, P(*i*-C_6H_5)$_3$], 130.2 [d, $^4J_{PC}$ = 2.9, P(*p*-C_6H_5)$_2$], 129.7 [s, *C*CH(CH_3)$_2$], 129.4 [d, $^3J_{PC}$ = 11.3, pend-P(*m*-C_6H_5)$_2$ or pend-P(*m*-$C_6'H_5$)$_2$], 128.4 [d, $^3J_{PC}$ = 10.5, pend-P(*m*-$C_6'H_5$)$_2$ or pend-P(*m*-C_6H_5)$_2$], 129.1 [d, $^3J_{PC}$ = 11.2, RuP(*m*-C_6H_5)$_2$], 128.4 [d, $^3J_{PC}$ = 10.5, RuP(*m*-C_6H_5)$_3$], 128.3 [d, $^3J_{PC}$ = 11.9, RuP(*m*-$C_6'H_5$)$_2$], 114.8 (m, RuPPh_2*CC*PPh_2), 100.3 (s, CH_3–*C*), 99.0 (s, *o*-$CH_3C_6H_4$ and *o*-$CH_3C'_6H_4$), 91.0 (d, $^2J_{PC}$ = 9.6, *m*-$CH_3C_6H_4$), 90.4 (d, $^2J_{PC}$ = 9.4, *m*-$CH_3C_6'H_4$), 31.3 [s, *C*H(CH_3)$_2$], 21.6 [s, CH(*C*H_3)$_2$ or CH(*C*′H_3)$_2$], 21.1 [s, CH(*C*′H_3)$_2$ or CH(*C*H_3)$_2$], 15.5 (s, *C*H_3–C_6H_4). ^{31}P{^{1}H} NMR ($CDCl_3$): δ = 24.2 (d, $^2J_{PP}$ = 55.1, 1 P, Ru–*P*Ph_3), 1.0 (dd, $^3J_{PP}$ = 3.2, $^2J_{PP}$ = 55.1, 1 P, Ru–*P*Ph_2), –31.7 (d, $^3J_{PP}$ = 4.9, 1 P, pend-*P*Ph_2), –144.4 (sept, $^1J_{PF}$ = 712.7, 1 P, *P*F_6). IR (nujol, cm^{-1}): $\tilde{\nu}_{\nu(CC)}$ = 2105 (w). ESI-MS (MeOH) positive ion: *m*/*z* = 533 (15) [M – PPh_2CCPPh_2]$^+$, 665 (20) [M – PPh_3]$^+$, 927 (100) [M]$^+$. ESI-MS^2 (+927): *m*/*z* = 665 [M – PPh_3]$^+$. ESI-MS negative ion: *m*/*z* = 145 [PF_6]$^-$. $C_{54}H_{49}ClF_6P_4Ru$·0.75CH_2Cl_2 (1136.09): calcd. C 57.88, H 4.48; found C 57.54, H 4.53.

Preparation of [(η^6-*p*-Cymene)RuCl(PPh_3)(η^1-PPh_2CCPPh_2-BH_3)]PF_6 (7B): To a solution of **7** (0.150 g, 0.12 mmol) in THF (25 mL, –78 °C) a solution of BH_3·THF in THF (0.10 mL of ca. 1.2 M, 0.12 mmol) was added dropwise. The solution was then stirred for 1 h. The solvent was removed in vacuo as the solution warmed to room temperature, the residue washed with diethyl ether (2 × 20 mL) and then dried in vacuo. Yield: 0.095 g (78%). ^{1}H NMR ($CDCl_3$): δ = 8.03 [dd, $^3J_{HH}$ = 7.6, $^3J_{PH}$ = 12.4, 2 H, RuP(*o*-C_6H_5)$_2$CCPPh_2], 7.94 [dd, $^3J_{HH}$ = 7.4, $^3J_{PH}$ = 12.3, 2 H, pend-P(*o*-C_6H_5)$_2$], 7.88 [dd, $^3J_{HH}$ = 7.4, $^3J_{PH}$ = 12.1, 2 H, pend-P(*o*-C_6H_5')$_2$], 7.1–7.7 (m, 27 H, P*Ph*), 7.00 [td, $^4J_{PH}$ = 2.6, $^3J_{HH}$ = 7.6, 2 H, RuP(*m*-C_6H_5')$_2$CCPPh_2], 5.73–5.80 [m, 1 H, *o*-$CH_3C_6H_4'$ {^{31}P@δ = 5.7} δ = 5.77, d, $^3J_{HH}$ = 6.3], 5.70 (d, $^3J_{HH}$ = 6.1, 1 H, *m*-$CH_3C_6H_4$), 5.30–5.23 [m, 1 H, *o*-$CH_3C_6H_4$ {^{31}P@δ = 24.5} δ = 5.26, d, $^3J_{HH}$ = 6.5], 5.07 (d, $^3J_{HH}$ = 6.1, 1 H, *m*-$CH_3C_6H_4'$), 2.80 [sept, $^3J_{HH}$ = 6.9, 1 H, C*H*(CH_3)$_2$], 0.8–1.8 [br., 3 H, B*H*$_3$; {^{11}B@δ = –37.7} δ = 1.46, d, $^2J_{PH}$ = 16.2], 1.1–1.4 [m, $^3J_{HH}$ = 6.4, 9 H, CH(C*H*$_3$)$_2$, CH(C*H*$_3'$)$_2$ and C*H*$_3$–C_6H_4]. ^{13}C{^{1}H} NMR ($CDCl_3$, –50 °C): δ = 128–134 (poorly resolved, P*Ph*), 133 [pend-P(*o*-C_6H_5)$_2$ and pend-P(*o*-$C_6'H_5$)$_2$], 132 [RuP(*o*-C_6H_5)$_3$], 131 [*C*CH(CH_3)$_2$], 129 [RuP(*m*-$C_6'H_5$)$_2$CCPPh_2], 125.6 (m, RuPPh_2*CC*PPh_2), 99 (CH_3–*C*), 99 (*o*-$CH_3C_6H_4$), 97 (*o*-$CH_3C_6'H_4$), 91 (*m*-$CH_3C_6'H_4$), 90 (*m*-$CH_3C_6H_4$), 31.6 [s, *C*H(CH_3)$_2$], 21.8 [s, CH(*C*H_3)$_2$ or CH(*C*′H_3)$_2$], 21.5 [s, CH(*C*′H_3)$_2$ or CH(*C*H_3)$_2$], 15.1 (s, *C*H_3–C_6H_4). ^{31}P{^{1}H} NMR ($CDCl_3$): δ = 24.5 (d, $^2J_{PP}$ = 55.1, 1 P, Ru–*P*Ph_3), 7.8 (br., 1 P, *P*–BH_3), 5.7 (d, $^3J_{PP}$ = 55.1, 1 P, Ru–*P*Ph_2), –144.3 (sept, $^1J_{PF}$ = 712.7, 1 P, *P*F_6). ^{11}B{^{1}H} NMR ($CDCl_3$): δ = –37.7 (br). IR (nujol, cm^{-1}): $\tilde{\nu}$ = ν(CC) not observed; ν(BH) 2393 (br). ESI-MS (MeOH) positive ion: *m*/*z* = 927 (100) [M – BH_3]$^+$, 941 (10) [M]$^+$. ESI-MS (CH_2Cl_2) positive ion: *m*/*z* = 927 (14) [M – BH_3]$^+$, 941 (100) [M]$^+$. ESI-MS^2 (+941): *m*/*z* = 927 [M – BH_3]$^+$. ESI-MS^3 (+941; +927): *m*/*z* = 665 [M – PPh_3 – BH_3]$^+$. ESI-MS (CH_2Cl_2) negative ion: *m*/*z* = 145 (100) [PF_6]$^-$.

Preparation of [(η^6-*p*-Cymene)$RuCl_2$(η^1-$PPh_2CH_2PPh_2BH_3$)] (1B): To a solution of [(η^6-*p*-cymene)$RuCl_2$(η^1-dppm)] (0.08 g, 0.116 mmol) in CH_2Cl_2 (5 mL, 0 °C) a solution of BH_3·THF in THF (0.12 mL of ca. 1 M, 0.12 mmol) was added dropwise. The solution was then warmed to room temperature and stirred for 30 minutes. The product was isolated as an orange powder, following concentration of the solution in vacuo and the addition of excess hexane. Yield: 0.06 g (78%). Orange crystals suitable for X-ray diffraction were obtained by slow diffusion of pentane into a chloroform solution of **1B** at room temperature. ^{1}H NMR ($CDCl_3$): δ = 7.9–8.1 [m, 4 H, RuP(*o*-C_6H_5)$_2$; {^{31}P@δ = 22.7} δ = 8.02, d, $^3J_{HH}$ = 7.1], 7.35–7.44 [m, 4 H, P(*o*-C_6H_5)$_2$$BH_3$; {^{31}P@$\delta$ = 11.9} δ = 7.39, d, $^3J_{HH}$ = 7.2], 7.1–7.35 [m, 12 H, P(*m*,*p*-C_6H_5)$_2$], 5.23 (d, $^3J_{HH}$ = 5.6, 2 H, *o*-$CH_3C_6H_4$), 5.11 (d, $^3J_{HH}$ = 6.0, 2 H, *m*-$CH_3C_6H_4$), 3.92 (t, $^2J_{PH}$ = 10.4, 2 H, P–C*H*$_2$–P), 2.49 [sept, $^3J_{HH}$ = 6.9, 1 H, C*H*(CH_3)$_2$], 1.79 (s, 3 H, C*H*$_3$–C_6H_4), 0.87 [d, $^3J_{HH}$ = 6.9, 6 H, CH(C*H*$_3$)$_2$], 0.1–1.2 [br., 3 H, B*H*$_3$; {^{11}B@δ = –38.4} δ = 0.70, d, $^2J_{PH}$ = 15.6]. ^{13}C{^{1}H} NMR ($CDCl_3$): δ = 133.9 [d, $^2J_{PC}$ = 9.7, RuP(*o*-C_6H_5)$_2$], 131.4 [d, $^2J_{PC}$ = 9.6, P(*o*-C_6H_5)$_2$$BH_3$], 131.2 [d, $^4J_{PC}$ = 2.5, RuP(*p*-C_6H_5)$_2$], 130.5 [d, $^4J_{PC}$ = 2.3, P(*p*-C_6H_5)$_2$-BH_3], 129.5–130.5 [m, P(*i*-C_6H_5)$_2$], 128.5 [d, $^3J_{PC}$ = 10.2, P(*m*-C_6H_5)$_2$], 127.9 [d, $^3J_{PC}$ = 10.3, P(*m*-C_6H_5)$_2$], 108.7 [s, *C*CH(CH_3)$_2$], 94.3 (s, CH_3–*C*), 90.2 (d, $^2J_{PC}$ = 4.3, *o*-$CH_3C_6H_4$), 85.5 (d, $^2J_{PC}$ = 6.0, *m*-$CH_3C_6H_4$), 30.0 [s, *C*H(CH_3)$_2$], 21.4 [s, CH(*C*H_3)$_2$], 17.2 (s, *C*H_3–C_6H_4), 16.7 (dd, $^1J_{PC}$ = 19.4, $^1J_{PC}$ = 24.3, P–*C*H_2–P). ^{31}P{^{1}H} NMR ($CDCl_3$): δ = 22.7 (d, $^2J_{PP}$ = 29.2, 1 P, Ru–*P*), 11.9 (br., 1 P, *P*–BH_3). ^{11}B{^{1}H} NMR ($CDCl_3$): δ = –38.4 (br). IR (nujol, cm^{-1}): $\tilde{\nu}_{\nu(BH)}$ = 2419 (br), 2389 (br). $C_{35}H_{39}BCl_2P_2Ru$·CH_2Cl_2 (789.36): calcd. C 54.78, H 5.24; found C 55.24, H 5.26.

Preparation of [(η^6-*p*-Cymene)$RuCl_2$(η^1-$PPh_2CH_2CH_2PPh_2BH_3$)] (8B): To a solution of dppe (0.104 g, 0.26 mmol) in CH_2Cl_2 (10 mL, 0 °C) a solution of [(η^6-*p*-cymene)$RuCl_2$]$_2$ (0.100 g, 0.16 mmol) in CH_2Cl_2 (5 mL) followed, ca. 1 min later, by a solution of BH_3·THF in THF (0.16 mL of ca. 1.2 M, 0.19 mmol)] were added rapidly. The solution was then warmed to room temperature and stirred for 1 h. The solvent was then removed in vacuo, and the residue extracted with toluene (25 mL). Further [(η^6-*p*-cymene)$RuCl_2$(μ-dppe)-$RuCl_2$(η^6-*p*-cymene)] could be separated from the reaction mixture by recrystallisation from CH_2Cl_2/pentane, at –20 °C. Purification of the remaining material by preparative TLC (acetone/CH_2Cl_2, 1:11), extracting the first orange band with acetone, give the pure

product. Yield: 0.02 g (19%/BH_3, 10%/Ru). Orange crystals suitable for X-ray diffraction were obtained by recrystallisation of **8B** from CH_2Cl_2/pentane at –20 °C. ^{1}H NMR ($CDCl_3$): δ = 7.68–7.78 [m, 4 H, RuP(*o*-C_6H_5)$_2$; {^{31}P@δ = 23.6} m′], 7.58–7.68 [m, 4 H, P(*o*-C_6H_5)$_2$$BH_3$; {^{31}P@$\delta$ = 18.2} m′], 7.58–7.8 [m, 12 H, P(*m*,*p*-C_6H_5)$_2$], 5.19 (d, $^3J_{HH}$ = 5.7, 2 H, *o*-$CH_3C_6H_4$), 5.12 (d, $^3J_{HH}$ = 6.0, 2 H, *m*-$CH_3C_6H_4$), 2.7–2.9 [m, 2 H, $CH_2PPh_2BH_3$; {^{31}P@δ = 23.6} δ = 2.77, $^3J_{HH}$ = 4.2, $^2J_{PC}$ = 12.9], 2.58 [sept, $^3J_{HH}$ = 6.9, 1 H, $CH(CH_3)_2$], 2.2–2.4 [m, 2 H, $RuPPh_2CH_2$; {^{31}P@δ = 18.2} δ = 2.29, $^3J_{HH}$ = 3.9, $^2J_{PC}$ = 13.2], 1.90 (s, 3 H, CH_3–C_6H_4), 1.01 [d, $^3J_{HH}$ = 6.9, 6 H, $CH(CH_3)_2$], 0.3–1.2 [br., 3 H, BH_3; {^{11}B@δ = –40.6} δ = 0.80, d, $^2J_{PH}$ = 16.0]. ^{13}C{^{1}H} NMR ($CDCl_3$): δ = 133.6 [d, $^1J_{PC}$ = 42.6, P(*i*-C_6H_5)$_2$], 133.2 [d, $^2J_{PC}$ = 9.0, RuP(*o*-C_6H_5)$_2$], 132.2 [d, $^1J_{PC}$ = 9.4, P(*o*-C_6H_5)$_2$$BH_3$], 131.1 [d, $^4J_{PC}$ = 2.2, P(*p*-C_6H_5)$_2$$BH_3$], 130.9 [d, $^4J_{PC}$ = 2.2, RuP(*p*-C_6H_5)$_2$], 128.5–129.1 [obscured, P(*i*-C_6H_5)$_2$], 128.7 [d, $^2J_{PC}$ = 10.0, P(*m*-C_6H_5)$_2$], 128.6 [d, $^1J_{PC}$ = 9.5, P(*m*-C_6H_5)$_2$], 109.5 [s, *C*$CH(CH_3)_2$], 95.7 (s, CH_3–*C*), 89.8 (d, $^2J_{PC}$ = 4.0, *o*-$CH_3C_6H_4$), 85.9 (d, $^2J_{PC}$ = 5.6, *m*-$CH_3C_6H_4$), 30.1 [s, *C*$H(CH_3)_2$], 21.8 [s, $CH(CH_3)_2$], 21.7 (d, $^1J_{PC}$ = 29.8, *C*$H_2PPh_2BH_3$), 20.0 (d,, $^1J_{PC}$ = 36.9), 17 $RuPPh_2CH_2$.6 (s, *C*H_3–C_6H_4). ^{31}P{^{1}H} NMR ($CDCl_3$): δ = 23.6 (d, $^3J_{PP}$ = 42.8, 1 P, Ru–*P*), 18.2 (br., 1 P, *P*–BH_3). ^{11}B{^{1}H} NMR ($CDCl_3$): δ = –40.6 (br). IR (nujol, cm^{-1}): $\tilde{\nu}_{v(BH)}$ = 2370 (br).

Preparation of [(η^6-*p*-Cymene)$RuCl_2$(η^1-$PPh_2C_5H_4FeC_5H_4PPh_2$-BH_3)] (9B): To a solution of dppf (0.145 g, 0.26 mmol) in CH_2Cl_2 (10 mL, 0 °C ice slurry) a solution of [(η^6-*p*-cymene)$RuCl_2$]$_2$ (0.100 g, 0.16 mmol) in CH_2Cl_2 (5 mL) followed, ca. 1 min later, by a solution of BH_3·THF in THF (0.16 mL of ca. 1.2 M, 0.19 mmol) were added. The solution was then warmed to room temperature and stirred for 1 h, and the solvent was removed in vacuo. Extraction of the solid with toluene (40 mL) followed by recrystallisation of this extract from CH_2Cl_2/pentane at –20 °C gave the product as a orange solid. Yield: 0.11 g (61% /BH_3, 37% /Ru). Further purification is achieved by preparative TLC (acetone/CH_2Cl_2, 1:10), extracting the first orange band with acetone. ^{1}H NMR ($CDCl_3$): δ = 7.7–7.8 [m, 4 H, RuP(*o*-C_6H_5)$_2$; {^{31}P@δ = 18.5} δ = 7.77, dd, $^4J_{HH}$ = 1.4, $^3J_{HH}$ = 7.7], 7.3–7.5 [m, 16 H, P(*o*-C_6H_5)$_2$$BH_3$ and P(*m*,*p*-C_6H_5)$_2$], 5.17 (d, $^3J_{HH}$ = 5.8, 2 H, *o*-$CH_3C_6H_4$), 5.10 (d, $^3J_{HH}$ = 6.1, 2 H, *m*-$CH_3C_6H_4$), 4.45–4.50 [m, 2 H, (*m*-C_5H_4)PPh_2BH_3], 4.32–4.37 [m, 2 H, (*o*-C_5H_4)PPh_2BH_3], 4.10–4.15 [m, 2 H, RuP-Ph_2(*o*-C_5H_4)], 4.80–4.86 [m, 2 H, $RuPPh_2$(*m*-C_5H_4)], 2.53 [sept, $^3J_{HH}$ = 6.9, 1 H, *C*$H(CH_3)_2$], 1.78 (s, 3 H, CH_3–C_6H_4), 0.94 [d, $^3J_{HH}$ = 7.0, 6 H, $CH(CH_3)_2$], 0.7–1.5 [br., 3 H, BH_3; {^{11}B@δ = –38.5} δ = 1.13, d, $^2J_{PH}$ = 16.4]. ^{13}C{^{1}H} NMR ($CDCl_3$): δ = 136.8 [d, $^1J_{PC}$ = 47.1, RuP(*i*-C_6H_5)$_2$], 133.8 [d, $^2J_{PC}$ = 9.5, RuP(*o*-C_6H_5)$_2$], 132.5 [d, $^2J_{PC}$ = 9.7, P(*o*-C_6H_5)$_2$$BH_3$], 131.0 [d, $^1J_{PC}$ = 59.2, P(*i*-C_6H_5)$_2$$BH_3$], 130.9 [d, $^4J_{PC}$ = 2.3, RuP(*p*-C_6H_5)$_2$], 130.2 [d, $^3J_{PC}$ = 2.1, P(*p*-C_6H_5)$_2$], 128.4 [d, $^3J_{PC}$ = 10.2, P(*m*-C_6H_5)$_2$], 127.7 [d, $^3J_{PC}$ = 9.7, P(*m*-C_6H_5)$_2$], 109.7 [s, *C*$CH(CH_3)_2$], 95.1 (s, CH_3–*C*), 90.4 (d, $^2J_{PC}$ = 4.2, *o*-$CH_3C_6H_4$), 85.9 (d, $^2J_{PC}$ = 6.0, *m*-$CH_3C_6H_4$), 76.53 [d, $^3J_{PC}$ = 7.4, (*m*-C_5H_4)PPh_2BH_3], 76.49 [d, $^2J_{PC}$ = 10.0, $RuPPh_2$(*o*-C_5H_4)], 73.3 [d, $^3J_{PC}$ = 9.8, $RuPPh_2$(*m*-C_5H_4)], 72.5 [d, $^2J_{PC}$ = 7.5, (*o*-C_5H_4)PPh_2BH_3], 69.0 [d, $^1J_{PC}$ = 67.4, $RuPPh_2$(*i*-C_5H_4)], 29.9 [s, *C*$H(CH_3)_2$], 21.7 [s, $CH(CH_3)_2$], 17.0 (s, *C*H_3–C_6H_4); the signal of (*i*-C_5H_4)PPh_2BH_3 was not unambiguously located. ^{31}P{^{1}H} NMR ($CDCl_3$): δ = 18.5 (s, 1 P, Ru–*P*), 15.8 (br., 1 P, *P*–BH_3). ^{11}B{^{1}H} NMR ($CDCl_3$): δ = –38.5 (br). IR (nujol, cm^{-1}): $\tilde{\nu}_{v(BH)}$ = 2373 (br).

Preparation of 1,4-$BrC_6H_4PPh_2BH_3$: To a solution of 1,4-$BrC_6H_4PPh_2$ (1.50 g, 4.40 mmol) in THF (50 mL, 0 °C) a solution of BH_3·THF in THF (3.7 mL, ca. 1.2 M, 4.40 mmol) was added dropwise. The solution was warmed to room temperature after 15 minutes and then concentrated to approximately 30 mL. The product was then precipitated by the addition of hexane, filtered, washed with hexane (ca. 20 mL) and dried in vacuo. Yield 1.30 g (83%). ^{1}H NMR ($CDCl_3$): δ = 7.4–7.7 [m, 14 H, BH_3PPh_2(C_6H_4Br)], 0.8–1.8 [br., 3 H, BH_3 {^{11}B@δ = –38.0} δ = 1.27, d, $^2J_{PH}$ = 16.3]. ^{31}P{^{1}H} NMR ($CDCl_3$): δ = 20.8 (d, $^1J_{PB} \approx$ 55). ^{11}B{^{1}H} NMR ($CDCl_3$): δ = –38.0 (d, $^1J_{PB} \approx$ 55). IR (nujol, cm^{-1}): $\tilde{\nu}_{v(BH)}$ = 2385 (br).

Preparation of 1,4-$PPh_2C_6H_4PPh_2BH_3$: To a solution of 1,4-$BrC_6H_4PPh_2BH_3$ (0.60 g, 1.69 mmol) in THF (30 mL, –78 °C) a solution of BuLi in hexane (1.1 mL, ≈ 1.6 M, 1.7 mmol) followed by $ClPPh_2$ (0.32 mL, 1.78 mmol) were added dropwise. The solution was stirred for a further 20 minutes and then warmed to room temperature. The product was precipitated as a white solid by concentration and then collected by filtration, washed with methanol (2 × 10 mL) and dried in vacuo. Yield 0.61 g (73%). ^{1}H NMR ($CDCl_3$): δ = 7.4–7.7 [m, 14 H, BH_3PPh_2(C_6H_4Br)], 0.8–1.8 [br., 3 H, BH_3 {^{11}B@δ = –38.0} δ = 1.27, d, $^2J_{PH}$ = 16.3]. ^{31}P{^{1}H} NMR ($CDCl_3$): δ = 20.8 (br., 1 P, PPh_2BH_3), –4.9 (s, 1 P, pend-PPh_2). ^{11}B{^{1}H} NMR ($CDCl_3$): δ = –38.0 (br). IR (nujol, cm^{-1}): $\tilde{\nu}_{v(BH)}$ = 2398 (br).

Preparation of [(η^6-*p*-Cymene)$RuCl_2$(η^1-1,4-$PPh_2C_6H_4PPh_2BH_3$)] (10): A solution of [(η^6-*p*-cymene)$RuCl_2$]$_2$ (0.20 g, 0.33 mmol) and 1,4-$PPh_2C_6H_4PPh_2BH_3$ (0.30 g, 0.65 mmol) in CH_2Cl_2 was stirred at room temperature for 1 h. After concentration to ca. 25 mL the product was precipitated with hexane. The orange solid was collected by filtration, washed with hexane (3 × 10 mL) and dried in vacuo. Yield: 0.41 g (82%). ^{1}H NMR ($CDCl_3$): δ = 7.79–7.93 [m, 6 H, $RuPPh_2$(*o*-$C_6H_4PPh_2BH_3$) and RuP(*o*-C_6H_5)$_2$; {^{31}P@δ = 24.9} δ = 7.89, dd, 2 H, $RuPPh_2$(*o*-$C_6H_4PPh_2BH_3$), $^3J_{PH}$ = 1.2, $^3J_{HH}$ = 8.3 Hz; δ = 7.85, dd, 4 H, RuP(*o*-C_6H_5)$_2$, $^4J_{HH}$ = 1.5, $^3J_{HH}$ = 7.9], 7.52–7.6 [m, 4 H, P(*o*-C_6H_5)$_2$$BH_3$; {^{31}P@$\delta$ = 20.5} δ = 7.56, dd, $^4J_{HH}$ = 1.4, $^3J_{HH}$ = 8.3], 7.3–7.52 [m, 14 H, $RuPPh_2$(*m*-$C_6H_4PPh_2BH_3$) and P(*m*,*p*-C_6H_5)$_2$], 5.22 (d, $^3J_{HH}$ = 6.1, 2 H, *m*-$CH_3C_6H_4$), 5.02 (d, $^3J_{HH}$ = 5.6, 2 H, *o*-$CH_3C_6H_4$), 2.85 [sept, $^3J_{HH}$ = 6.9, 1 H, *C*$H(CH_3)_2$], 1.88 (s, 3 H, CH_3–C_6H_4), 1.11 [d, $^3J_{HH}$ = 6.9, 6 H, $CH(CH_3)_2$], 0.6–1.76 [br., 3 H, BH_3; {^{11}B@δ = –38.1} δ = 1.23, d, $^2J_{PH}$ = 16.3]. ^{13}C{^{1}H} NMR ($CDCl_3$): δ = 137.1 [dd, $RuPPh_2$(*i*-$C_6H_4PPh_2BH_3$), $^4J_{PC}$ = 2.3, $^1J_{PC}$ = 44.1], 134.4 [m, RuP-Ph_2(*o*-$C_6H_4PPh_2BH_3$)], 134.3 [d, $^2J_{PC}$ = 9.7, RuP(*o*-C_6H_5)$_2$], 133.4 [d, $^1J_{PC}$ = 45.0, P(*i*-C_6H_5)$_2$], 132.1 [m, $RuPPh_2$(*m*-$C_6H_4PPh_2BH_3$)], 131.2 [dd, $^4J_{PC}$ = 2.2, $^1J_{PC}$ = 56.2, $RuPPh_2$(*p*-$C_6H_4PPh_2BH_3$)], 131.4 [d, $^4J_{PC}$ = 2.3, P(*p*-C_6H_5)$_2$$BH_3$], 130.7 [d, $^4J_{PC}$ = 2.2, RuP(*p*-C_6H_5)$_2$], 128.8 [d, $^3J_{PC}$ = 10.3, P(*m*-C_6H_5)$_2$], 128.4 [d, $^1J_{PC}$ = 58.2, P(*i*-C_6H_5)$_2$], 128.3 [d, $^3J_{PC}$ = 9.9, P(*m*-C_6H_5)$_2$], 111.4 [d, $^2J_{PC}$ = 3.4, *C*$CH(CH_3)_2$], 96.2 (s, CH_3–*C*), 89.0 (d, $^2J_{PC}$ = 3.0, *o*-$CH_3C_6H_4$), 87.3 (d, $^2J_{PC}$ = 5.5, *m*-$CH_3C_6H_4$), 30.3 [s, *C*$H(CH_3)_2$], 21.8 [s, $CH(CH_3)_2$], 17.8 (s, *C*H_3–C_6H_4). ^{31}P{^{1}H} NMR ($CDCl_3$): δ = 24.9 (s, 1 P, Ru–*P*), 20.5 (br., 1 P, *P*–BH_3). ^{11}B{^{1}H} NMR ($CDCl_3$): δ = –38.1 (br). IR (nujol, cm^{-1}): $\tilde{\nu}_{v(BH)}$ = 2372 (br). $C_{40}H_{41}BCl_2PRu \cdot {}^1/_3CH_2Cl_2$ (794.81): calcd. C 60.95, H 5.28; found C 60.78, H 5.19.

X-ray Crystallography: Relevant details about the structure refinements are given in Table 2 and Table 3. Selected geometrical parameters are included in the captions of Figure 3, Figure 4, Figure 6, Figure 7, Figure 10, Figure 11 and Figure 12. Data collection for the X-ray structure determinations for compounds **2**, **3**, **5**, **2B** and **8B** were performed with a four-circle Kappa goniometer equipped with an Oxford Diffraction KM4 Sapphire CCD at 140(2) K. For compounds **6** and **1B** diffraction data were collected with a mar345 IPDS instrument at 140(2) K. Data reduction was performed using CrysAlis RED.[25] Structure solutions were solved by direct methods using SIR92 (**8B**),[26] SIR97 (**2**, **6**, **1B**),[27] or

SHELXTL[28] (**3**, **5**), or by Patterson interpretation using SHELXTL (**2B**).[28] Structure refinements were performed using the SHELXTL software package for all compounds. An empirical absorption correction (DELABS)[29] was applied to all data sets except for that of **3**. The structures of all compounds were refined using full-matrix least-squares on F^2 with the exception of **3**, which was refined using full-matrix-block least-squares on F^2. All non-hydrogen atoms were refined anisotropically, with hydrogen atoms placed in calculated positions using the riding model with the exception of the BH hydrogen atoms, which were located on the Fou-

Table 2. Crystal data and details of the structure determinations for **2**, **3**, **5** and **6**.

	2	**3**	**5**	**6**
CCDC	280165	280166	280167	280168
Chemical formula	$C_{36}H_{36}Cl_2P_2Ru$	$C_{35}H_{36}Cl_2OP_2Ru{\cdot}1.5CHCl_3$	$C_{36}H_{34}Cl_2P_2Ru{\cdot}3CHCl_3$	$C_{46}H_{50}Cl_2P_2Ru_2{\cdot}2CHCl_3$
Formula mass	702.56	885.60	1058.65	1176.58
Crystal system	triclinic	triclinic	monoclinic	monoclinic
Space group	$P\bar{1}$	$P\bar{1}$	$P2_1/n$	$P2_1/n$
a [Å]	10.5479(7)	15.4477(11)	15.9347(10)	12.710(4)
b [Å]	12.5815(13)	22.0211(12)	11.5059(10)	11.4016(18)
c [Å]	12.8323(14)	25.5063(12)	25.7256(15)	17.294(5)
α	81.579(9)°	72.314(5)°		
β	82.482(8)°	85.723(5)°	98.777(5)°	101.06(2)°
γ	85.270(7)°	88.496(5)°		
V [Å^3]	1666.6(3)	8243.4(8)	4661.4(6)	2459.6(11)
Z	2	8	4	2
$D_{calcd.}$ (g cm^{-3})	1.400	1.427	1.509	1.589
F(000)	720	3592	2128	1188
μ [mm^{-1}]	0.750	0.907	1.063	1.147
Temp. [K]	140(2)	140(2)	140(2)	140(2)
Wavelength [Å]	0.71073	0.71073	0.71073	0.71073
Measd. reflns.	9849	49686	26017	14479
Unique reflns.	5142	25535	7835	4336
Unique reflns. [$I > 2\sigma(I)$]	3659	12102	5586	3513
No. of data / restraints / parameters	5142 / 0 / 373	25535 / 90 / 1706	7835 / 12 / 518	4336 / 3 / 284
R[a] [$I > 2\sigma(I)$]	0.0463	0.0686	0.0593	0.0452
wR_2[a] (all data)	0.1066	0.1991	0.1708	0.1023
GoF[b]	0.923	0.912	1.060	1.065

[a] $R = \Sigma||F_o| - |F_c||/\Sigma|F_o|$, $wR_2 = \{\Sigma[w(F_o^2 - F_c^2)^2]/\Sigma[w(F_o^2)^2]\}^{1/2}$. [b] GoF = $\{\Sigma[w(F_o^2 - F_c^2)^2]/(n - p)\}^{1/2}$ where n is the number of data and p is the number of parameters refined.

Table 3. Crystal data and details of the structure determinations for **1B**, **2B** and **8B**.

	1B	**2B**	**8B**
CCDC	280169	280170	280171
Empirical formula	$C_{35}H_{39}BCl_2P_2Ru{\cdot}CHCl_3$	$C_{36}H_{39}BCl_2P_2Ru{\cdot}CH_2Cl_2$	$C_{36}H_{41}BCl_2P_2Ru{\cdot}2CH_2Cl_2$
Formula mass	823.75	801.32	888.26
Crystal system	monoclinic	monoclinic	triclinic
Space group	$C2/c$	$P2_1/c$	$P\bar{1}$
a [Å]	39.660(17)	14.5111(8)	8.7826(6)
b [Å]	11.024(3)	16.6311(10)	14.5506(15)
c [Å]	18.413(10)	17.1449(9)	16.754(2)
α			81.354(9)°
β	111.29(7)°	114.847(5)°	88.283(8)°
γ			80.581(7)°
V [Å^3]	7501(6)	3754.7(4)	2088.2(4)
Z	8	4	2
$D_{calcd.}$ (g cm^{-3})	1.459	1.418	1.413
F(000)	3360	1640	908
μ [mm^{-1}]	0.885	0.813	0.862
Temp. [K]	140(2)	140(2)	140(2)
Wavelength [Å]	0.71073	0.71073	0.71073
Measd. reflns.	23670	21520	12575
Unique reflns.	6594	6295	6465
Unique reflns. [$I > 2\sigma(I)$]	3801	5483	4171
No. of data / restraints / parameters	6594 / 74 / 450	6295 / 6 / 420	6465 / 12 / 447
R[a] [$I > 2\sigma(I)$]	0.0781	0.0390	0.0516
wR_2[a] (all data)	0.2331	0.1057	0.1326
GoF[b]	0.993	1.050	0.937

[a] $R = \Sigma||F_o| - |F_c||/\Sigma|F_o|$, $wR_2 = \{\Sigma[w(F_o^2 - F_c^2)^2]/\Sigma[w(F_o^2)^2]\}^{1/2}$. [b] GoF = $\{\Sigma[w(F_o^2 - F_c^2)^2]/(n - p)\}^{1/2}$ where n is the number of data and p is the number of parameters refined.

rier difference map and then constrained to equal BH bond lengths and H–B–H angles. Disorder in the *p*-cymene ring in complex **1B** was satisfactorily modeled by splitting the isopropyl moiety (with constrained geometries) over two sites, constraining the ring and restraining the atomic displacement parameters of the ring using SIMU and ISOR commands. Some of the solvent molecules in **3**, **5** and **6** were constrained or split over multiple sites. It was also necessary to restrain the atomic displacement parameters of some atoms in the structures of **3**, **5**, and **8B**. Graphical representations of the structures were made with Diamond.[30] CCDC-280165–280171 contain the supplementary crystallographic data for this paper (see Table 2 and Table 3). These data can be obtained free of charge from The Cambridge Crystallographic Data Centre via www.ccdc.cam.ac.uk/data_request/cif.

Acknowledgments

We thank the New Zealand Foundation for Research, Science and Technology for a Top Achiever Doctoral Fellowship (A. B. C.), the EPFL and the Swiss National Science Foundation for financial support.

[1] F. A. Cotton, G. Wilkinson, C. A. Murillo, M. Bochman, *Advanced Inorganic Chemistry*, 6th ed., John Wiley & Sons, New York, **1999**.

[2] For examples see: a) L. H. Pignolet (Ed.), *Homogeneous Catalysis with Metal Phosphine Complexes*, Plenum Press, New York, **1983**; b) R. Noyori, *Asymmetric Catalysis in Organic Synthesis*, Wiley, New York, **1994**; c) P. A. Chaloner, M. A. Esteruelas, F. Joó, L. A. Oro, *Homogeneous Hydrogenation*, Kluwer Academic Press, Dordrecht, **1994**; d) T. Naota, H. Takaya, S.-I. Murahashi, *Chem. Rev.* **1998**, *98*, 2599–2660; e) O. W. N. M. van Leeuwen, P. C. J. Kamer, J. N. H. Reek, P. Dierkes, *Chem. Rev.* **2000**, *100*, 2741–2769.

[3] For examples see: a) A. Santos, J. López, J. Montoya, P. Noheda, A. Romero, A. M. Echavarren, *Organometallics* **1994**, *13*, 3605–3615; b) J. W. Benson, R. L. Keiter, E. A. Keiter, A. L. Rheingold, G. P. A. Yap, V. V. Mainz, *Organometallics* **1998**, *17*, 4275–4281 and references cited therein; c) J. E. Mague, M. S. Balakrishna, *Polyhedron* **1996**, *15*, 4259–4268; d) E. Louattani, J. Suades, K. Urtiaga, M. I. Arriortua, X. Solans, *Organometallics* **1996**, *15*, 468–471; e) N. E. Leadbeater, J. Lewis, P. R. Raithby, A. J. Edwards, *J. Organomet. Chem.* **1997**, *545–546*, 567–572; f) Y. Yang, K. A. Abboud, L. McElwee-White, *Dalton Trans.* **2003**, 4288–4296; g) W.-Y. Yeh, C.-I. Li, S.-M. Peng, G.-H. Lee, *J. Organomet. Chem.* **2004**, *689*, 105–110.

[4] a) P. McQuade, N. P. Rath, L. Barton, *Inorg. Chem.* **1999**, *38*, 5468–5470 and references cited therein; b) P. McQuade, R. E. K. Winter, N. P. Rath, L. Barton, *Inorg. Chim. Acta* **2005**, *358*, 1545.

[5] a) A. W. Coleman, D. F. Jones, P. H. Dixneuf, C. Brisson, J.-J. Bonnet, G. Lavigne, *Inorg. Chem.* **1984**, *23*, 952–956; b) A. W. Coleman, H. Zhang, S. G. Bott, J. L. Atwood, P. H. Dixneuf, *J. Coord. Chem.* **1987**, *16*, 9–17; c) D. K. Gupta, A. N. Sahay, D. S. Pandey, N. K. Jha, P. Sharma, G. Espinosa, A. Cabrera, M. C. Puerta, P. Valerga, *J. Organomet. Chem.* **1998**, *568*, 13–20.

[6] For examples see: a) C. J. Adams, M. I. Bruce, B. W. Skelton, A. H. White, *J. Organomet. Chem.* **1992**, *423*, 83–96; b) E. Stein, F. Y. Fujiwara, *J. Organomet. Chem.* **1996**, *525*, 31–37; c) P. M. van Calcar, M. M. Olmstead, A. L. Balch, *Inorg. Chim. Acta* **1998**, *270*, 28–33.

[7] For recent examples see: a) C. Daguenet, P. J. Dyson, *Catal. Commun.* **2003**, *4*, 153–157; b) P. J. Dyson, D. J. Ellis, W. Henderson, G. A. Laurenczy, *Adv. Synth. Catal.* **2003**, *345*, 216–221; c) C. Daguenet, R. Scopelliti, P. J. Dyson, *Organometallics* **2004**, *23*, 4849–4857; d) C. Daguenet, P. J. Dyson, *Organometallics* **2004**, *23*, 6080–6083.

[8] a) T. J. Geldbach, P. J. Dyson, *J. Am. Chem. Soc.* **2004**, *126*, 8114–8115; b) T. J. Geldbach, M. R. H. Brown, R. Scopelliti, P. J. Dyson, *J. Organomet. Chem.* **2005**, Online Advanced Article: April 29.

[9] M.-E. Moret, A. B. Chaplin, A. K. Lawrence, R. Scopelliti, P. J. Dyson, *Organometallics* **2005**, *24*, 4039–4048.

[10] a) J. M. Brunel, B. Faure, M. Maffei, *Coord. Chem. Rev.* **1998**, *178–180*, 665–698; b) B. Carboni, L. Monnier, *Tetrahedron* **1999**, *55*, 1197–1248.

[11] R. Macías, N. P. Rath, L. Barton, *Angew. Chem. Int. Ed.* **1999**, *38*, 162–164.

[12] M. Ingleson, N. J. Patmore, G. D. Ruggiero, C. G. Frost, M. F. Mahon, M. C. Wills, A. S. Weller, *Organometallics* **2001**, *20*, 4434–4436.

[13] N. Merle, G. Koicok-Köhn, M. F. Mahon, C. G. Frost, G. D. Ruggerio, A. S. Weller, M. C. Willis, *Dalton Trans.* **2004**, 3883–3892.

[14] F. Estevan, P. Lahuerta, J. Latorre, A. Sanchez, C. Sieiro, *Polyhedron* **1987**, *6*, 473–478.

[15] I. Moldes, E. de la Encarnación, J. Ros, Á. Alvanez-Larena, J. F. Piniella, *J. Organomet. Chem.* **1998**, *566*, 165–174.

[16] Alternatively, [(η^6-*p*-cymene)$RuCl_2$(η^1-dppm)] can be quantitatively converted to [(η^6-*p*-cymene)$RuCl_2$(η^1-dppmO)] by treatment with H_2O_2 in THF. ^{1}H and ^{31}P NMR spectroscopic data were in agreement with the literature data.[17]

[17] J. W. Faller, B. P. Patel, M. A. Albrizzio, M. Curtis, *Organometallics* **1999**, *18*, 3096–3104.

[18] Refluxing a solution of [(η^6-*p*-cymene)$_2Ru_2(\mu$-Cl)$_3$]PF_6 and dppa (1.5 equivalents) in CH_2Cl_2 for 2.5 h leads to a mixture containing [(η^6-*p*-cymene)$RuCl_2$(η^1-dppa){(μ-dppa)$RuCl_2$(η^6-*p*-cymene)}]$^+$ {^{31}P NMR ($CDCl_3$): δ = 29.0 (s, 1 P, $RuCl_2$*P*), 22.4 (d, $^2J_{PP}$ = 61, 1 P, Ru*P*Ph_2CCPPh_2), 2.4 (d, $^2J_{PP}$ = 62, 1 P, Ru*P*Ph_2CCPPh_2RuCl_2), –30.7 (d, $^3J_{PP}$ = 5, 1 P, pend-*P*). ESI-MS (CH_2Cl_2) positive ion: *m*/*z* = +1365 [M]$^+$}. Although small amounts can be purified by preparative TLC (acetone/CH_2Cl_2, 1:24), this complex undergoes an equilibration reaction leading to a mixture containing [(η^6-*p*-cymene)RuCl(η^1-dppa)$_2$]$^+$ {^{31}P NMR ($CDCl_3$): δ = 11.9 (s, 1 P, RuCl*P*), –31.3 (s, 1 P, pend-*P*). ESI-MS (CH_2Cl_2) positive ion: *m*/*z* = +1059 [M]$^+$} and [(η^6-*p*-cymene)RuCl{(μ-dppa)$RuCl_2$(η^6-*p*-cymene)}$_2$]$^+$ {^{31}P NMR ($CDCl_3$): δ = 24.4 (br., 1 P, Ru*P*), 8.3 (br., 1 P, Ru*P*). ESI-MS (CH_2Cl_2) positive ion: *m*/*z* = +1671 [M]$^+$}.

[19] Determined by ^{31}P NMR of an aliquot taken from the solution after 2 h, the solvent removed in vacuo and then the solid redissolved in $CDCl_3$.

[20] P. J. Dyson, J. S. McIndoe, *Inorg. Chima Acta* **2003**, *354*, 68.

[21] M. Herberhold, H. Yan, W. Milius, *J. Organomet. Chem.* **2000**, *598*, 142–149.

[22] M. A. Bennett, T. N. Huang, T. W. Matheson, A. K. Smith, *Inorg. Synth.* **1982**, *21*, 74.

[23] M. A. Bennett, A. K. Smith, *J. Chem. Soc., Dalton Trans.* **1974**, 233.

[24] R. A. Baldwin, M. T. Cheng, *J. Org. Chem.* **1967**, *32*, 1572–1577.

[25] Oxford Diffraction Ltd., Abingdon, Oxfordshire, U. K., **2003**.

[26] A. Altomare, M. C. Burla, G. Camalli, G. Cascarano, C. Giacovazzo, A. Guagliardi, G. Polidori, *J. Appl. Crystallogr.* **1994**, *27*, 435–436.

[27] A. Altomare, M. C. Burla, M. Camalli, G. L. Cascarano, C. Giacovazzo, A. Guagliardi, A. G. G. Moliterni, G. Polidori, R. Spagna, *J. Appl. Crystallogr.* **1999**, *32*, 115–119.

[28] G. M. Sheldrick, *SHELXTL*; University of Göttingen, Germany, **1997**; Bruker AXS, Inc., Madison, WI, **1997**.

[29] N. Walker, D. Stuart, *Acta Crystallogr., Sect. A* **1983**, *39*, 158.

[30] Diamond 3.0a; Crystal Impact GbR, Bonn, Germany, **2004**.

Received: August 5, 2005
Published Online: October 25, 2005

